IS-T 1789

Characterization of Organosulfur Monolayer Formation at Gold Elec. trodes

by

Tani Woods, Nina

MS Thesis submitted to Iowa State University

Ames Laboratory, U.S. DOE

Iowa State University

Ames, Iowa 50011

Date Transmitted: August 1, 1996

PREPARED FOR THE U.S. DEPARTMENT OF ENERGY

UNDER CONTRACT NO. W-7405-Eng-82.

DISCLAIMER

AVAILABILITY:

To DOE and DOE contractors: Office of Scientific and Technical Information
P.O. Box 62
Oak Ridge, TN 37831

prices available from: (615) 576-8401
FTS: 626-8401

To the public: National Technical Information Service
U.S. Department of Commerce
5285 Port Royal Road
Springfield, VA 22161

TABLE OF CONTENTS

1. GENERAL INTRODUCTION

The design of chemically modified interfaces has increasingly become a popular topic in analytical chemistry in recent years because of the abundance and importance of many detection processes that occur at interfaces [1]. Of the major efforts in this field, the modification of electrode surfaces by the assembly of organic thin films onto the electrode has sparked great interest [2, 3]. The bulk of studies in this area centers on the design and function of the electrode surface.

Among the many types of organic films, covalently-attached organosulfur monolayers have attracted a great deal of attention. The foundation of organosulfur monolayer chemistry was laid by the pioneering work of Nuzzo and Allara [4]. In a communication in 1983, they utilized a number of techniques, including contact angle, ellipsometry and infrared spectroscopy, to show that cyclic organic disulfides formed stable monolayer films at gold electrodes. These results also demonstrated their structural coherence and ease of preparation and, most importantly, stimulated interest in the study of sulfur-based monomolecular films as models for interfacial processes.

We have focused our interest on the fundamental characterization of spontaneously adsorbed organosulfur monolayers. This introductory chapter presents general aspects of monolayer preparation and characterization, followed by a few examples that illustrate the range of applications of these films.

Preparation

Spontaneously adsorbed organosulfur monolayers are formed by immersing the substrate in a dilute solution of precursor molecules in an organic solvent. Substrates include gold, copper [5, 6] and silver [7-9]. However, gold is widely used because of its inertness towards most contaminant adsorption and oxide formation. These substrates are usually prepared by the evaporation of gold onto glass, mica or silicon substrates, yielding microscopically rough surfaces which can be smoothed if necessary by annealing. Studies using STM have shown that the surface of annealed gold on mica consists mostly of smooth Au(111) terraces [10].

The monolayer itself can be classified as having three main components, shown in Figure 1.1. It is important to note that this picture is idealized and does not show chain defects and other probable anomalies.

The head group is crucial to the chemisorption process. Formation of spontaneously adsorbed monolayers is initiated by the strong affinity of the head group for the substrate. The bonding energy of the slightly polar covalent bond between sulfur and gold is on the order of 30-40 kcal/mol [2].

The cohesive interactions between the methylene chains also are of importance to the formation of the monolayer, influencing its packing and barrier properties. A well-packed alkanethiolate monolayer typically consists of extended conformational sequences of alkyl chains tilted at 30^0 from surface normal, which allows the chains to maximize attractive chain-chain interactions [11].

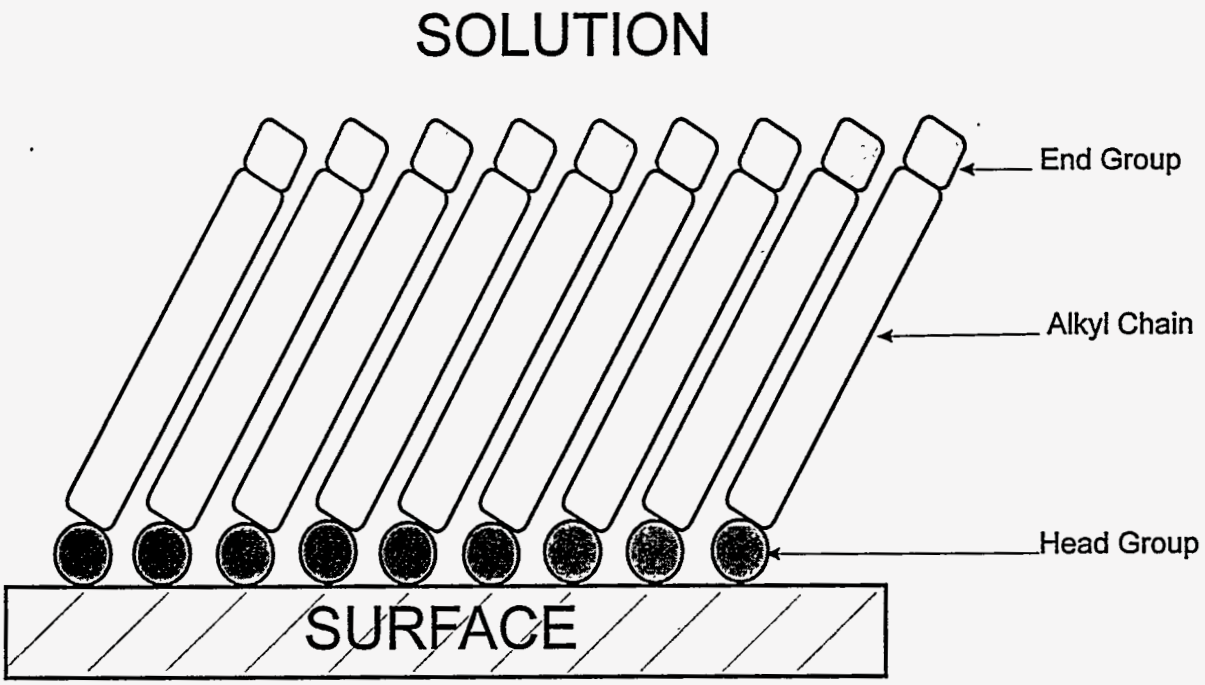

Figure 1.1: Idealized schematic diagram of a monolayer at a surface

The density of these chains has been estimated at 4×10^{14} chains/cm^2 by tritium labeling studies [12]. Generally, monolayers formed with longer alkyl chains are more crystalline-like in character than shorter chains.

The end group, because of its proximity to the interface of the surface and solution, dominates the interfacial properties and can be varied depending on the applications. The size of the end group also determines the packing of the monolayer. In one study, the measurement of contact angles using hexadecane for a series of ethers of the form $HS(CH_2)_{16}O(CH_2)_nCH_3$ were identical to that of pure alkanethiols, indicating that the end groups were so tightly packed that the oxygen in the ether linkage was inaccessible [13].

Characterization

As the utility of organosulfur monolayers continues to become more extensive, techniques for characterizing these films have advanced. X-ray photoelectron spectroscopy (XPS) has been used to probe the composition, thickness and gold-sulfur bonding of these monolayers. In a number of independent analyses, these experiments have shown that the sulfur species assembled on a gold electrode from alkanethiol precursors are thiolates, presumably from the cleavage of the S-H bond [14-16].

Probe microscopies have developed rapidly in the characterization of these monolayers. Scanning tunneling microscopy (STM) [10, 17] and atomic force microscopy (AFM) [18, 19] studies have demonstrated that the sulfur atoms of long-

chain alkanethiolates conform to a ($\sqrt{3}$ x $\sqrt{3}$)R 30^0 structure at an Au(111) surface and are predicted to reside in the threefold hollow sites of the Au(111) surface [20].

Electrochemical methods have been widely employed to study adsorbate-adsorbate and adsorbate-substrate interactions. Organosulfur monolayers can be desorbed by a one-electron process from the surface by applying a cathodic voltage sweep [10,21]. A recent study demonstrated the dependence of the cathodic peak potential (E_p) on chain length [10]. Results revealed that as chain length increases, E_p shifts negatively by ~20 mV per methylene unit. Reductive desorption is also ideal for investigating redox-active end groups such as ferrocene [21].

Monolayer coverages are frequently determined by measuring the charge under the wave during the reductive desorption of the monolayer. The surface coverage of several methyl-terminated alkanethiols has been measured to be 9.3 ($\pm$0.6) x 10^{-10} mols/cm^2 [21]. This value correlates with the predicted surface coverage for the ($\sqrt{3}$ x $\sqrt{3}$)R 30^0 structure, which is 7.6 x 10^{-10} mole/cm^2 [10], after accounting for surface roughness.

Infrared reflection spectroscopy (IRS) and ellipsometry have been used to characterize the ordering and orientation of the alkyl chain structure. Prior experiments have shown that the chains are tilted roughly 30^0 from the surface normal and that the carbon-carbon bonds adopt an all-trans configuration [11]. These features have also been corroborated by x-ray diffraction [9] and Raman spectroscopy [22]. Infrared reflection spectroscopy has also been used to detect

and characterize terminal functional groups, especially those containing alcohols and carbonyl groups [23].

Applications

Organosulfur monolayers have been utilized for applications in many research areas. Besides their utility for studying fundamental electron transfer and interfacial processes, these films have been applied toward corrosion protection [2, 24], modeling of biological membranes [25] and immobilization of antibodies [26], just to name a few. This section describes a small portion of the many studies related to the application of these monolayers in sensors, lithography and electron transfer reactions.

Monolayers fabricated from organosulfur molecules show great promise in sensor applications and much effort has been devoted to studying the properties and reactivity of these systems for this purpose. In one instance, monolayers formed from mercaptopyridine isomers were exposed to anthraquinone-based adsorbates and studied by electrochemical methods [27]. Results of this study indicated that the monolayer film and the structure of the adsorbate play crucial roles in the adsorption process. There is continued effort in developing gas phase probes and recent experiments have investigated the bonding [28], reactivity [29], and film structure [30] of monolayers adsorbed from the vapor phase.

The inherently small dimensions of organosulfur molecules used to form monolayer films also makes them ideal for use in lithography. For example, small

areas of the monolayer may be removed to form trenches in which to lay the circuit. One method for the creation of the patterned surfaces involves the irradiation of a masked substrate with UV light to convert the exposed chemisorbed alkanethiolates to physisorbed alkanesulfonates which can be removed by rinsing. The resulting surface was probed by SIMS [31] and lateral force microscopy [32].

The tip of a scanning tunneling microscope or an atomic force microscope can also be used as a lithographic tool. In one such study, the etching of an alkanethiolate coated electrode with the tip of an STM created structures having dimensions from 50 nm up to 5.0 μm [33]. The highest resolution so far, on the order of 10 nm, was achieved by applying a large normal force to an atomic force microscope cantilever to etch the outer component of a bilayer [34].

The creation of monomolecular films has found widespread use in the study of electron transfer processes. The manipulation of monolayer architectures to facilitate electron transfer has been the subject of many studies. For example, ferrocene terminated alkanethiolate monolayers were used as models to study the fundamentals of electron transfer across an interface [35,36]. The experiment measured the forward and reverse rate constants, showing that the ferrocene groups behaved as kinetically homogeneous electron transfer sites. The electron tunneling parameters and the reorganizational energy of the system were also determined.

Organosulfur monolayers have also been widely used to facilitate the electron transfer of the protein cytochrome *c* [37,38]. In fact, the utility of organosulfur

monolayers for modifying electrodes was first demonstrated with cytochrome *c* [39], a large biomolecule which is known to have poor voltammetric responses due to unfolding of the protein at a bare electrode. These studies established that cytochrome *c* exhibited more reversible electrochemical behavior when exposed to gold electrodes modified with 4, 4' dipyridyl disulfide. Since then, several other organosulfur precursors have been evaluated for cytochrome *c* immobilization [40].

Unresolved Issues

Despite the voluminous data already collected about spontaneously adsorbed organosulfur monolayers, there are a number of issues that still remain unclear. Among the foremost of these issues is the interaction between the head-group and the substrate. There is still considerable debate as to the nature of the organosulfur species which forms on the surface. Another aspect of the chemisorption process which is unresolved is the mechanism by which the thiolate monolayers form and the byproducts that result from formation. This thesis is aimed at addressing some of the issues.

Thesis Organization

This thesis is organized into two papers. In the first paper, three analogous monolayer precursors are studied to determine their similarities and differences in the monolayer structure. A GC-MS analysis of products from the chemisorption process and open circuit potential measurements are used to derive possible mechanisms behind monolayer formation.

The second paper focuses on monolayers formed from thioctic acid, including its characterization and application to cytochrome *c* electrochemistry. Although thiols and disulfides have been extensively studied as monolayer precursors, thioctic acid is particularly interesting because the disulfide functionality of this asymmetric molecule is contained in a strained five-membered ring. Given the ring strain, steric bulk and asymmetry of the molecule, the study of these monolayers lend insight into the factors important for the formation of organosulfur monolayers. This thesis concludes with a general summary and directions for future studies.

References

1. Bard, A.J.; Abruna, H.D.; Chidsey, C.E.; Faulkner, L.R.;Feldberg, S.W.; Itaya, K.; Majda, M.; Melroy, O; Murray, R.W.; Porter, M.D.; Soriaga, M.P.; White, H.S. *J. Phys. Chem.* **1993**, *97*, 7147.

2. Ulman, A. *An Introduction to Ultrathin Organic Films: From Langmuir- Blodgett to Self Assembly*, Academic Press: Boston, **1991**.

3. Zhong, C.J.; Porter, M.D. *Anal. Chem.* **1995**, *67*, 709A.

4. Nuzzo, R.G.; Allara, D.L. *J. Am. Chem. Soc.* **1983**, *105*, 4481.

5. Stewart, K.R.; Whitesides, G.M.; Godfried, H.P.; Silvera, I.F. *Surf. Sci.* **1986**, *57*, 1381.

6. Laibinis, P.; Whitesides, G.M.; Allara, D. L.; Tao, Y.T.; Parikh, A.N.; Nuzzo, R.G. J. Am. Chem. Soc. 1991, 113, 7152.

7. Ulman, A. *J. Mat. Ed.* **1989**, *11*, 205.

8. Walczak, M. M.; Chung, C.; Stole, S.M.; Widrig, C.A.; Porter, M.D. J. AM. Chem. Soc. 1991, 113, 2370.

9. Bryant, M.A.; Pemberton, J. E. J. Am. Chem. Soc. 1991, 113, 3630.

10. Widrig, C.A.; Chung, C.; Porter, M.D. *J. Electroanal. Chem.* **1991**, *310*, 335.

11. Porter, M.D.; Bright, T.B.; Allara, D.L.; Chidsey, C.E.D. J. Am. Chem. Soc. 1987, 109, 3559.

12. Dubois, L.H. ; Nuzzo, R.G. *Annu. Rev. Phys. Chem.* **1992**, *43*, 437.

13. Bain, C.D.; Whitesides, G.M. *J. Am. Chem. Soc.* **1988**, *110*, 5897.

14. Bain, C.D.; Biebuyck, H.A. Whitesides, G.M. *Langmuir* **1989**, *5*, 723.

15. Nuzzo, R.G.; Zeharski, B.R.; Dubois, L.H. *J. Am. Chem. Soc.* **1987**, *109*, 733.

16. Nuzzo, R.G.; Fusco, F.A.; Allara, D.L. *J. Am. Chem. Soc.* **1987**, *109*, 2358.

17. McCarley, R.L.; Kim, Y.-T.; Bard, A.J. *J. Phys. Chem.* **1993**, *97*, 211.

18. Butt, H. J.; Seifert, K.; Bamberg, E. *J. Phys. Chem.* **1993**, *97*, 7316.

19. Alves, C.A.; Smith, E.L.; Porter, M.D. *J. Am. Chem. Soc.* **1992**, *114*, 1222.

20. Sellers, H.; Ulman, A.; Schnidman, Y.; Eilers, J.E. *J. Am. Chem. Soc.* **1993**, *115*, 9389.

21. Walczak, M.M.; Popenoe, D.D.; Deinhammer, R.S.; Lamp, B.D.; Chung, C.; Porter, M.D. *Langmuir* **1991**, *7*, 2687.

22. Fenter, P.; Eisenberger, P.; Liang, K.S. *Phys Rev. Lett.* **1993**, *70*, 2447.

23. Nuzzo, R.G.; Dubois, L. H.; Allara, D.L. *J. Am. Chem. Soc.* **1990**, *112*, 558.

24. Swalen, J.D.; Allara, D.L.; Andrade, J. D.; Chandross, E.A.; Garoff, S et. al. *Langmuir* **1987**, *3*, 932.

25. Holmes-Farley, S.R.; Bain, C.D.; Whitesides, G.M. *Langmuir* **1988**, *4*, 921.

26. Duan, C.; Meyerhoff, M.E. *Anal. Chem.* **1994**, *66*, 1369.

27. Jones, T.A.; Perez, G.P.; Johnson, B.J.; Crooks, R.M. *Langmuir* **1995**, *11*, 318.

28. Sun, L.; Kepley, L.J.; Crooks, R.M. *Langmuir* **1992**, *8*, 2101.

29. Xu, C.; Sun, L.; Kepley, L.J.; Crooks, R.M.; Ricco, A.J. *Anal Chem.* **1993**, *65*, 2102.

30. Chailapakul, O.; Sun, L.; Xu, C.; Crooks, R.M. *J. Am. Chem. Soc.* **1993**, *115*, 12459.

31. Tarlov, M.J.; Burgess, D.R.F.; Jr.; Gillen, G. *J. Am. Chem. Soc.* **1993**, *115*, 5305.

32. Frisbie, C.D.; Rozsnyai, L.F.; Noy, A.; Wrighton, M.S.; Lieber, C.M. *Science*, **1994**, *265*, 2071.

33. Ross, C.B.; Sun, L.; Crooks, R.M. *Langmuir* **1993**, *9*, 632.

34. Green, J.-B. D.; McDermott, M.T.; Porter, M.D.; Siperko, L.M. *J. Phys. Chem.* **1995**, *99*, 10960.

35. Chidsey, C.E.D.; Bertizzi, C.R.; Putvinski, T.M.; Miksce, A.M. *J. Am. Chem. Soc.* **1990**, *112*, 4301.

36. Chidsey, C.E.D. *Science* **1991**, *251*, 919.

37. Taniguchi, I.; Toyosawa, K.; Yamaguchi, H.; Yasukouchi, K. *J. Electroanal. Chem.* **1982**, *140*, 187.

38. Taniguchi, I.; Toyosawa, K.; Yamaguchi, H.; Yasukouchi, K. *J. Electroanal. Chem.* **1985**, *186*, 299.

39. Eddowes, M.J.; Hill, H.A.O *J. Chem. Soc. Chem. Commun.* **1977**, 771.

40. Allen, P.M.; Hill, A.O.; Watson, N.J. J. Electroanal. Chem. **1984**, *178*, 69.

2. CHARACTERIZATION OF THE CHEMISORPTION MECHANISMS FOR THE FORMATION OF ORGANO-SULFUR MONOLAYERS AT GOLD ELECTRODES DERIVED FROM THIOL, SULFIDE AND DISULFIDE PRECURSORS

A paper to be submitted to the *Journal of the American Chemical Society*

Nina T. Woods, Chuanjian Zhong, Marc D. Porter

Introduction

The extensive characterization of spontaneously adsorbed monolayers has been fueled mostly by their potential utility in many research areas [1]. Besides being of fundamental importance as model systems for studying interfacial processes, there are many other applications for spontaneously adsorbed monolayers, including chemical sensors [1-4], corrosion protection [5] and lithographic patterning [6-8]. Despite the numerous studies of these films, the binding chemistry of the head group to the substrate has not been well characterized. Among the issues that remain controversial are the nature of organosulfur species bound on the surface [9-10], the cleavage of adjacent bonds to the head group [11] and the number of electrons transferred in the process [12]. Yet, a better understanding of these formation processes is crucial in attaining better control of the architecture of these monolayers and for advancing desired applications.

Our group has been interested in the characterization of spontaneously adsorbed monolayers formed from different organosulfur precursors at gold surfaces [13-20]. An emphasis of this work is achieving a better understanding of the monolayer formation processes. To probe the mechanisms of monolayer formation, we compare in this paper monolayers derived from three related precursors, butanethiol, butyl sulfide and butyl disulfide. Our goal is to determine, first, if the same monolayer forms from all three precursors and second, the mechanisms and byproducts of the chemisorption process. The study encompasses a wide variety of techniques, including infrared reflection spectroscopy, electrochemistry, x-ray photoelectron spectroscopy and gas chromatography-mass spectrometry.

Experimental

Materials

Potassium hydroxide (99.99%), lithium perchlorate (95%), butanethiol (99%), butyl sulfide (96%) and butyl disulfide (98%) were all obtained from Aldrich Chemical Company and used as received. Gold powder (spherical, 2-8 micron, 99.95%) was purchased from Alfa Aesar and washed in pirhana solution (2:1 30% H_2O_2:concentrated H_2SO_4) in between each use. ***Caution:*** *Pirhana solution reacts violently with organic compounds. It should be handled with care and immediately disposed of after use.* The surface area of the gold powder was determined by BET measurements to be 0.27 m^2/g.

Preparation of Gold Electrodes

Electrodes were prepared by the resistive evaporation of gold onto either microscope glass slides (Fisher) or freshly cleaved mica using the following procedure.

Mica substrates (B&M Trading Company) were freshly cleaved into 75 mm x 25 mm sheets with a razor blade and passed under a stream of high purity argon prior to placement in the deposition chamber. Glass slides were cleaned in a 20% solution of Micro laboratory cleaner solution (Cole-Parmer), then rinsed with water and methanol and dried under a stream of argon prior to placement in the deposition chamber. The same procedure was used to deposit gold onto the glass substrates. However, the glass substrates were primed with 15 nm of chromium immediately prior to gold deposition.

The depositions were performed using an Edwards (Wilmington, MA) E306A vacuum coater operating at a base pressure of 10^{-6} torr. A nominal thickness of 300 nm of gold was deposited onto the mica surface at an evaporation rate of 0.3 - 0.4 nm/s.

Substrates were removed from the deposition chamber after cooling to ambient temperature. Upon removal, the Au/mica electrodes were annealed for 5 hours at 300°C in a muffle furnace under ambient atmosphere and allowed to cool to room temperature before storing in a dessicator. The annealing process produces a gold film which has predominantly Au(111) surface crystalinity [21,22,24].

Monolayer Preparation

Unless otherwise noted, gold electrodes were immersed in a 1 mM solution of the desired precursor in ethanolic solution for 18 hours. Just prior to use, the electrodes were rinsed thoroughly with absolute ethanol, then dried on a spin coater (Headway Research Inc., Garland, TX)

Electrochemical Measurements

Voltammetric experiments were performed in a conventional three-electrode electrochemical cell. The electrode area, defined by an inert elastomer O-ring, was 0.65 cm^2. A Pt coil electrode was used as a counter electrode. The reference electrode was a Ag/AgCl/sat'd KCl electrode; all potentials are reported with respect to this electrode. The supporting electrolyte was aqueous 0.5M KOH. Solutions were purged with high purity argon to remove oxygen for at least 5 minutes just before data collection.

Open circuit potential measurements were performed in the flow cell diagrammed in Figure 2.1. In these experiments, 0.2 mM solutions of a precursor was injected through the injection port of the valve into the flow cell containing only supporting electrolyte. The electrolyte solution was either 0.1 M KOH in absolute ethanol or 0.1 M $LiClO_4$ in absolute ethanol. Both these solutions enhance precursor solubility as well as provide adequate solution conductivity for the electrochemical measurements.

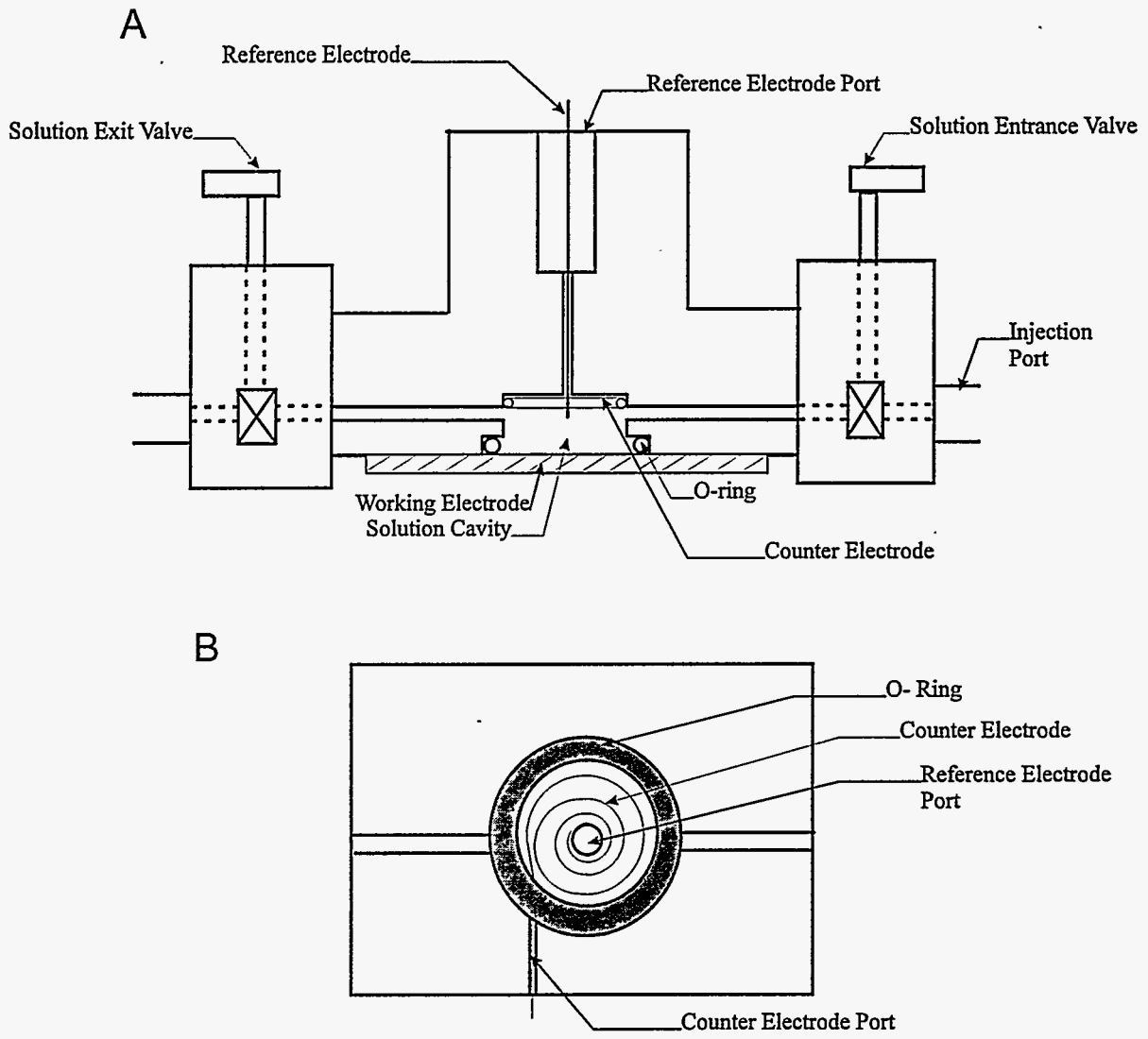

Figure 2.1: Schematic diagram of the electrochemical flow cell used in open circuit potential measurements. **A)** Side view; the electrode is mounted and sealed against the bottom of the cell. **B)** Bottom view; the counter electrode port allows a platinum wire to be inserted into the solution cavity and coiled just below and around the reference electrode port.

Electrochemical data was collected using a BAS (Bioanalytical Systems, West Lafayette, IN) model CV-27 potentiostat coupled with an X-Y recorder (The Recorder Company).

X-Ray Photoelectron Spectroscopy (XPS)

XPS spectra were acquired using a Physical Electronics (Eden Prairie, MN) Model 5500 surface analysis system equipped with a hemispherical analyzer, torroidal monochrometer, a multichannel detector and 300W Kα radiation (1486.6 eV) for excitation. The detection angle was 45^0 with respect to the surface normal.

Infrared Reflection Spectroscopy (IRS)

Data via IRS were obtained using a Nicolet Magna 750 FT-IR spectrometer with a liquid nitrogen-cooled HgCdTe detector. Light impinged on the samples with *p*-polarization at a 80^0 incident angle from the surface normal. The spectra are presented as -log (R/R_0) where R is the reflectance of the sample and R_0 is the reflectance of a reference octadecanethiolate-d_{37} monolayer on Au. Details concerning the preparation and handling of reference substrates have been given previously [23].

Gas Chromatography/Mass Spectrometry (GC-MS)

The GC-MS experiments were performed on a Finnigan Magnum mass spectrometer using electron impact for ionization and an ion trap mass analyzer. A DB-5 column (J&W Scientific) was used in the Varian gas chromatograph.

Separations were conducted by holding the temperature at 80^0 C for one minute after sample injection, followed by a temperature ramp of 10^0C/min to 220^0 C.

Results and Discussion

XPS Analysis

After monolayers were formed from butanethiol, butyl sulfide and butyl disulfide, XPS analysis was used to probe the nature of the gold-sulfur bond. The data in Figure 2.2 are XPS spectra for monolayers at Au(111) derived from of butanethiol, butyl sulfide and butyl disulfide in the S(2p) binding energy region. The positions of the bands in all three spectra at 161.9 eV and 163.2 eV, which respectively represent the $S(2p_{3/2})$ and $S(2p_{1/2})$ doublet, have previously been ascribed to a gold-bound thiolate species [14,25]. Thus, the similarities in peak position and shape for all three spectra suggest the presence of the same thiolate species. In other words, the comparable interactions between the sulfur and gold of the three monolayers, together with the lack of detectable bands for other oxidized or reduced species of sulfur, serves as evidence for the dominance of the gold-bound thiolate at the surface in all three cases. It follows that the S-H, S-C and S-S bonds of the thiol, sulfide and disulfide, respectively, are cleaved as a consequence of the chemisorption process.

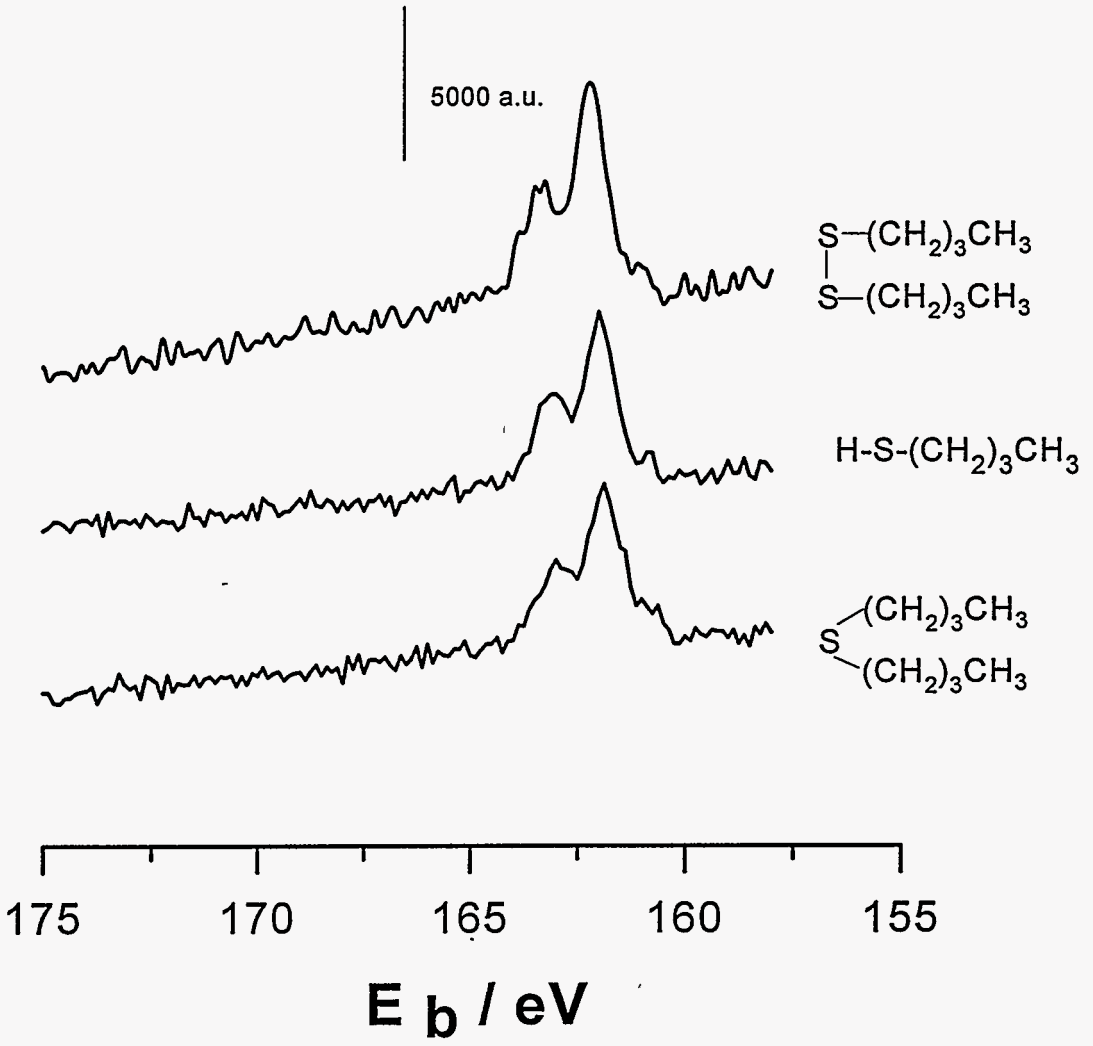

Figure 2.2: XPS spectra of monolayers formed from butanethiol, butyl sulfide and butyl disulfide in the S(2p) region

IRS Studies

The monolayers from the three different precursors were also examined by IRS. These spectra, shown in Figure 2.3, were taken in external reflectance mode. Although IRS does not provide information about the head group-substrate bonding, it allows us to characterize the general structure of the alkyl chains. The remarkable similarities in the C-H stretching region, such as the in-plane symmetric stretch of CH_3 at 2962 cm^{-1} and the asymmetric methylene stretch at 2926 cm^{-1}[15], demonstrate the close correspondence in the chain structures of the three monolayers. The slight broadening in the asymmetric stretch of CH_3 at 2872 cm^{-1} [15] of butyl sulfide and butanethiol-derived samples as compared to that of butyl disulfide is attributed to differences in packing density and order within the chains. We can thus conclude that the chains for monolayers formed from the thiol, sulfide and disulfide precursors are structurally similar.

Electrochemical Reductive Desorption

In previous reports, we have demonstrated that a monolayer can be desorbed from the gold surface by applying a sufficiently negative potential [16]. This electrochemical reductive desorption is described in equation 1 as:

$$Au\text{-}SR + e^- \rightarrow Au + RS^- \qquad (1)$$

The peak potential of the desorption wave is related to the strength of the bond between the substrate and the adsorbate, and interactions between neighboring

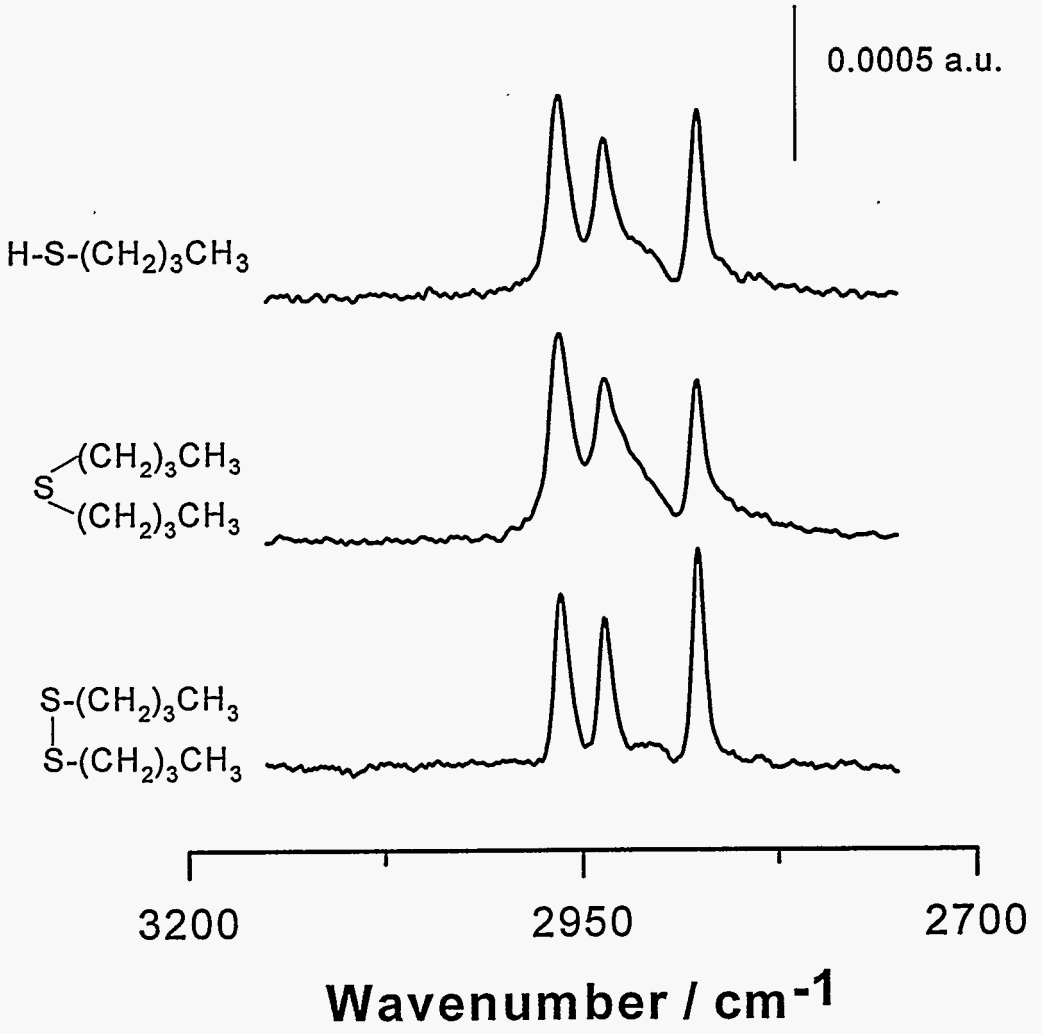

Figure 2.3: IRS spectra of monolayers formed from butanethiol, butyl sulfide and butyl disulfide in the C-H stretching region.

adsorbates. In addition, the surface coverage (Γ, mole/cm^2) of the monolayer can be determined by equation 2:

$$Q = nFA\Gamma \qquad (2)$$

where Q is charge in coulombs passed from the process in equation 1, n is the number of electrons transferred, F is Faraday's Constant and A is the electrode area in cm^2.To determine Q, the area under the desorption wave is integrated after a linear baseline approximation of the double layer charging current.

Figure 2.4 displays the cathodic voltammetric waves for monolayers derived from butanethiol, butyl sulfide and butyl disulfide at Au(111). The peak for the desorption wave for all three monolayers occurs at -0.78 V. This similarity, like the XPS data, argues that the interactions between sulfur and gold for all three systems are effectively indistinguishable. In addition, the surface coverages are also equivalent, with an average charge (Q) of 86$\pm$7 μC/cm^2 corresponding to a surface coverage of 9.1($\pm$ 1.1) x 10^{-10} moles/cm^2. After taking into account a roughness factor of 1.1 for Au/mica [16], this value is consistent with a theoretical surface coverage of 7.6 x 10^{-10} moles/cm^2 [16] that is expected for a ($\sqrt{3}$ x $\sqrt{3}$)R30^0 adlayer on a Au(111) surface. From the electrochemical data, we can conclude that monolayers formed from butanethiol, butyl sulfide and butyl disulfide have similar surface coverages and the bonding strength between sulfur and gold for all three species is comparable.

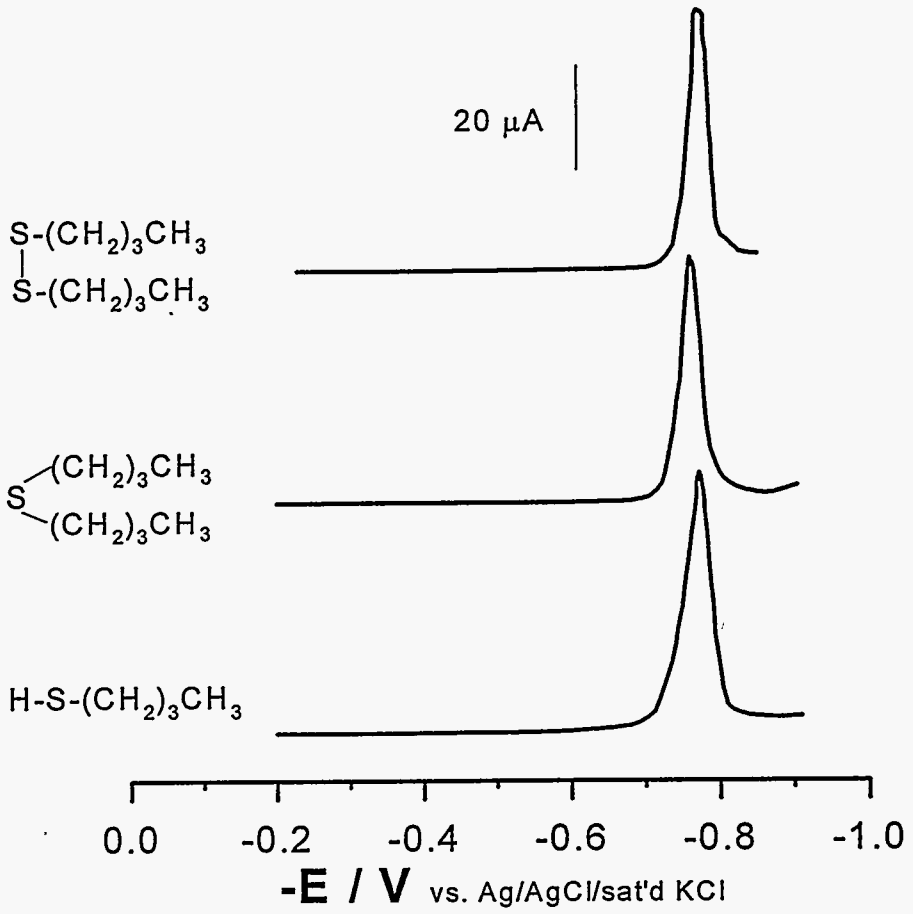

Figure 2.4: Cathodic waves for the reductive desorption of butanethiol, butyl sulfide and butyl disulfide at an Au/mica electrode. The electrolyte was 0.5M KOH and the scan rate was 50 mV/cm.

Open Circuit Potential Measurements

The monolayers formed from butanethiol and butyl sulfide were further subjected to open circuit potential measurements. The open circuit potential is the potential measured when there is effectively no current passing through the external circuit of the potentiostat. This potential is sensitive to the perturbation of the electrode/electrolyte interface by electronic or ionic charge transfer across the interface, or by dipole displacements and structural reorientations of species at the electrode-solution interface.

Figure 2.5A shows the open circuit potential transient at an Au/mica electrode as the monolayer forms from a dilute solution of butanethiol. Upon injection of 0.2 mmoles of butanethiol into a flow cell containing only electrolyte, the potential shifts negatively and reaches a maximum value of nearly -0.55V in ~30 s. The potential then begins to shift positively. The charge passed on the cathodic scan in a cyclic voltammogram collected after the open circuit measurement (Figure 2.5B) confirms that a full monolayer has been formed at the electrode over the course of the open circuit measurement.

We attribute the initial negative shift in potential to the donation of electrons from sulfur to gold - a process that imparts a net negative charge to the electrode surface. The return to more positive potentials is indicative of the discharge of the electrode. In contrast, we ascribe the discharging of the electrode to the loss of surface charge to a solution species. To investigate this possibility, we purged the

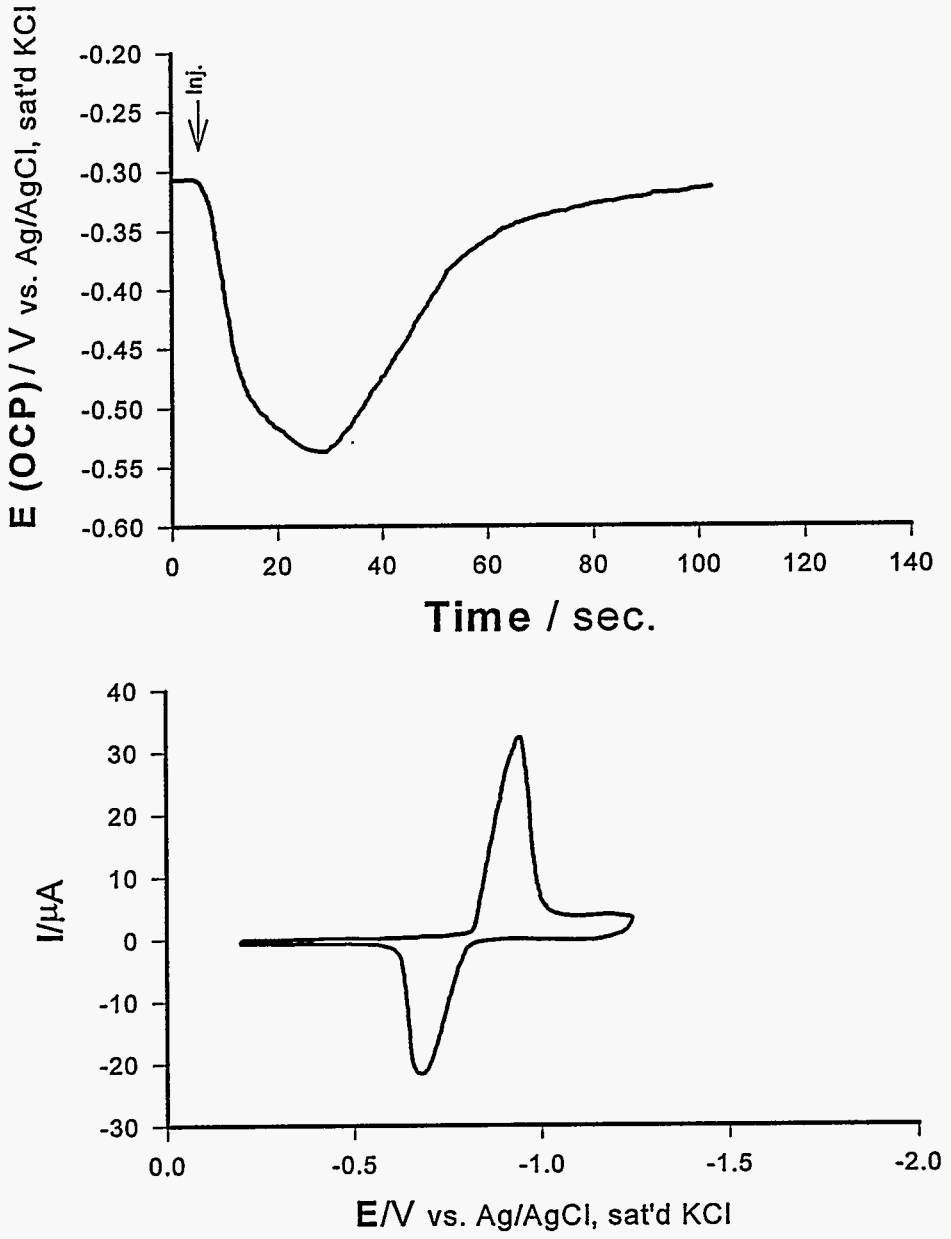

Figure 2.5: **A)** Open Circuit Potential Transient of $CH_3(CH_2)_3SH$. 0.2 mmoles of butanethiol is injected into 1 mL 0.1M KOH /absolute ethanol (10:90) **B)** A cyclic voltammogram is collected immediately after the open circuit potential measurement to verify that the monolayer is formed.

precursor solutions and the electrochemical cell extensively with argon gas to remove dissolved oxygen before injection of the butanethiol solution. Figure 2.6 compares the open circuit potential change with and without argon purging. The potential change for a control experiment using degassed supporting electrolyte devoid of butanethiol, shown in the inset of Figure 2.6A, shifts to a large positive value initially and approaches a lower, but still positive limiting value at long times. However, at the point of injection (t=0) of the deoxygenated butanethiol solution, the potential immediately shifts to more negative values. Without degasing of the solution, the open circuit potential shifts 300 mV more positively. In contrast, when the solution was degassed, the open circuit potential remained at a more negative potential, moving only ~ 50 mV more positively over time. The same set of responses are observed for an experiment using a solution of butyl sulfide, shown in Figure 2.6B. These results suggest that dissolved oxygen is one of the likely sources contributing to the discharging of the electrode. In summary, there is a net electron donation from S to Au for the adsorption process, followed by a discharging process through the reduction of a solution species.

Product Analysis

The previous experiments have shown that a butyl sulfide precursor solution forms thiolate species at the gold surface. If this is the case, it follows that the bond between sulfur and one of the carbons must cleave. The question then is what

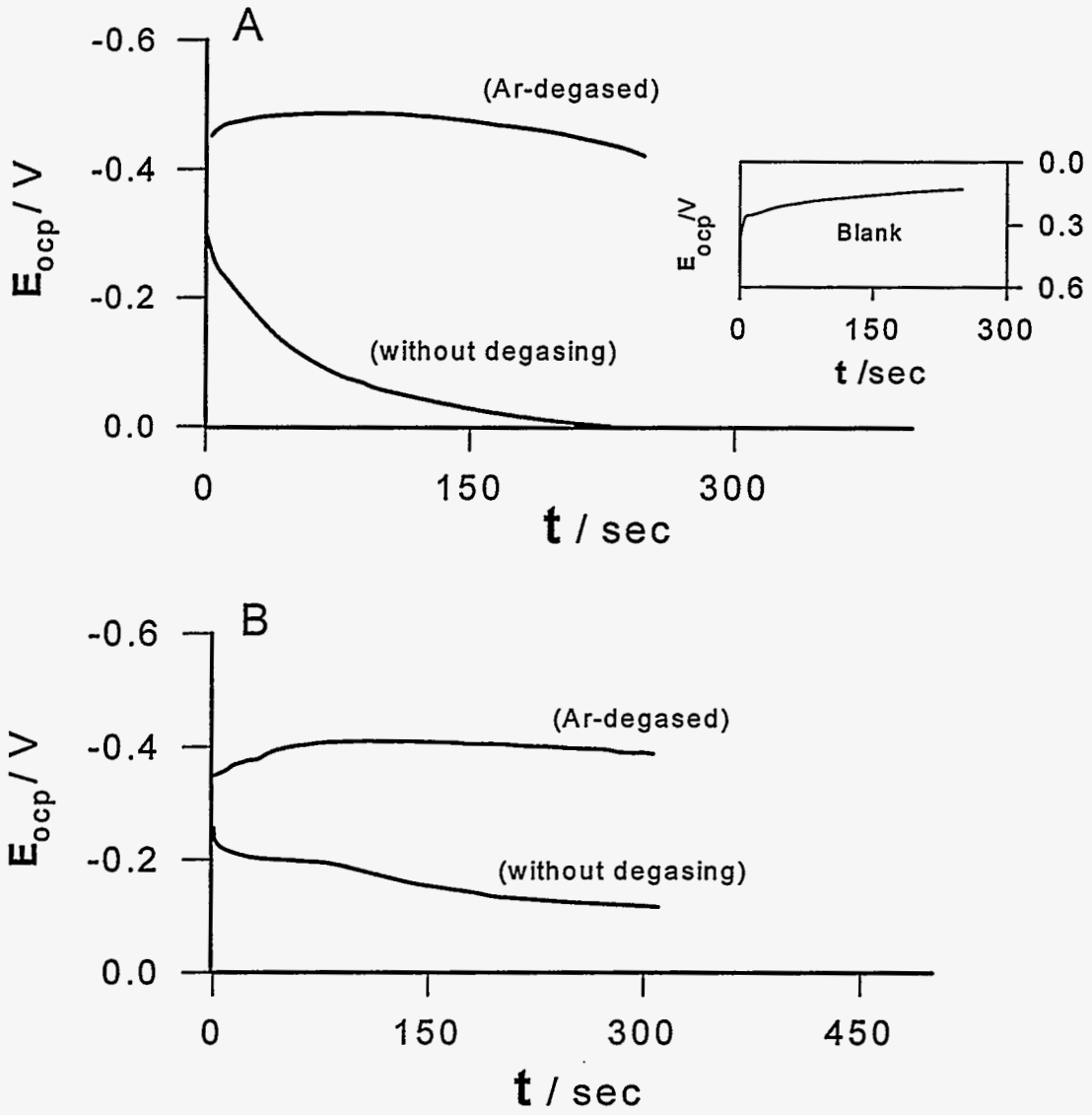

Figure 2.6: Open circuit potential change upon **A)** butanethiol and **B)** butyl sulfide chemisorption from ethanolic solution. The inset of Figure A is an experiment using a degassed solution devoid of butanethiol The supporting electrolyte was 0.1 M $LiClO_4$ and the precursor solutions used were 0.2 mM.

products are formed as a result of this bond cleavage? To determine the possible products of chemisorption, we employed GC-MS to analyze the solution used for monolayer formation. In this experiment, we immersed 5 grams of gold powder (surface area = 0.2-0.34 m^2/g) into 1 mM of butyl sulfide in ethanol. After stirring for 18 hours, the gold powder was allowed to settle and a 1-μL aliquot of the solution above the gold was collected and injected into the GC-MS. The GC-MS results are shown on Figure 2.7.

The chromatograph shows peaks for ethanol (t_r = 2:30 min) and the butyl sulfide (t_r = 6:30 min) starting material. There is a small peak at a retention time of 3 minutes that was not present in controls of butyl sulfide solutions without gold. The mass spectra of the peak at t_r = 3:00 min is shown in Figure 2.7A. Upon injecting a standard of butyraldehyde (Figure 2.7B) at the same concentration, the same mass spectra was obtained. Thus, the product of butyl sulfide chemisorption at gold is an aldehyde. These results further support the claim that oxygen-containing species is involved in the adsorption process of organosulfur molecules at the gold surface.

Conclusions

Based on the combined weight of the above experiments for the monolayers of butyl sulfide, we have derived a general proposed mechanism for the chemisorption of alkyl sulfides at gold electrodes, shown in Figure 2.8. A similar mechanism for alkyl thiols is shown in Figure 2.9. The schemes propose that when

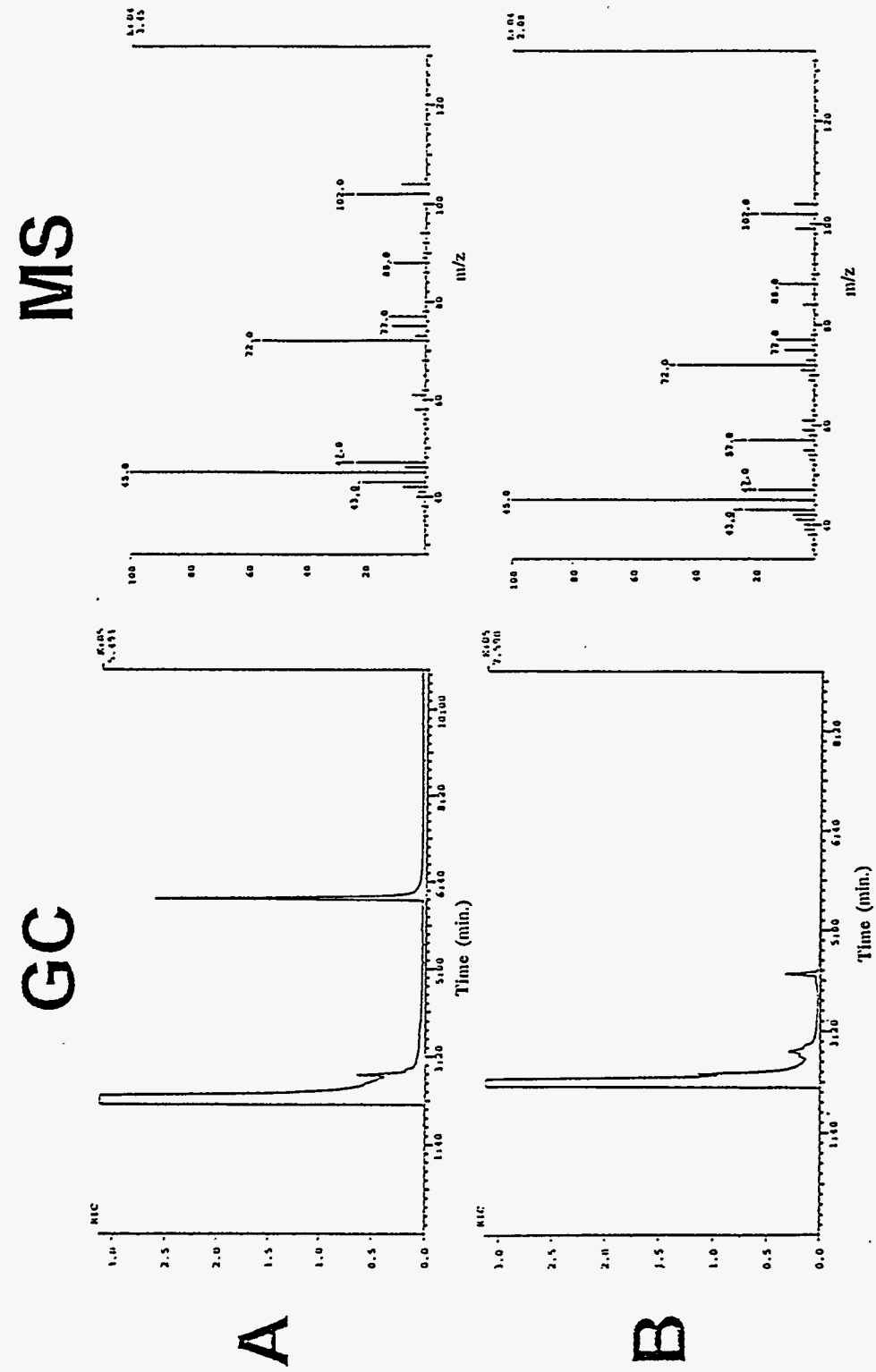

Figure 2.7: A) GC of the ethanolic solution after butyl sulfide monolayer formation at gold powder and the corresponding mass spectrum for the peak at t_r = 3 min. This peak was not detected in butyl sulfide/ethanol solutions devoid of gold powder. **B)** GC of a butyraldehyde standard and the corresponding mass spectrum for the peak at t_r = 3 min. The peak at t_r = 4:22 min is a trimer of butyraldehyde.

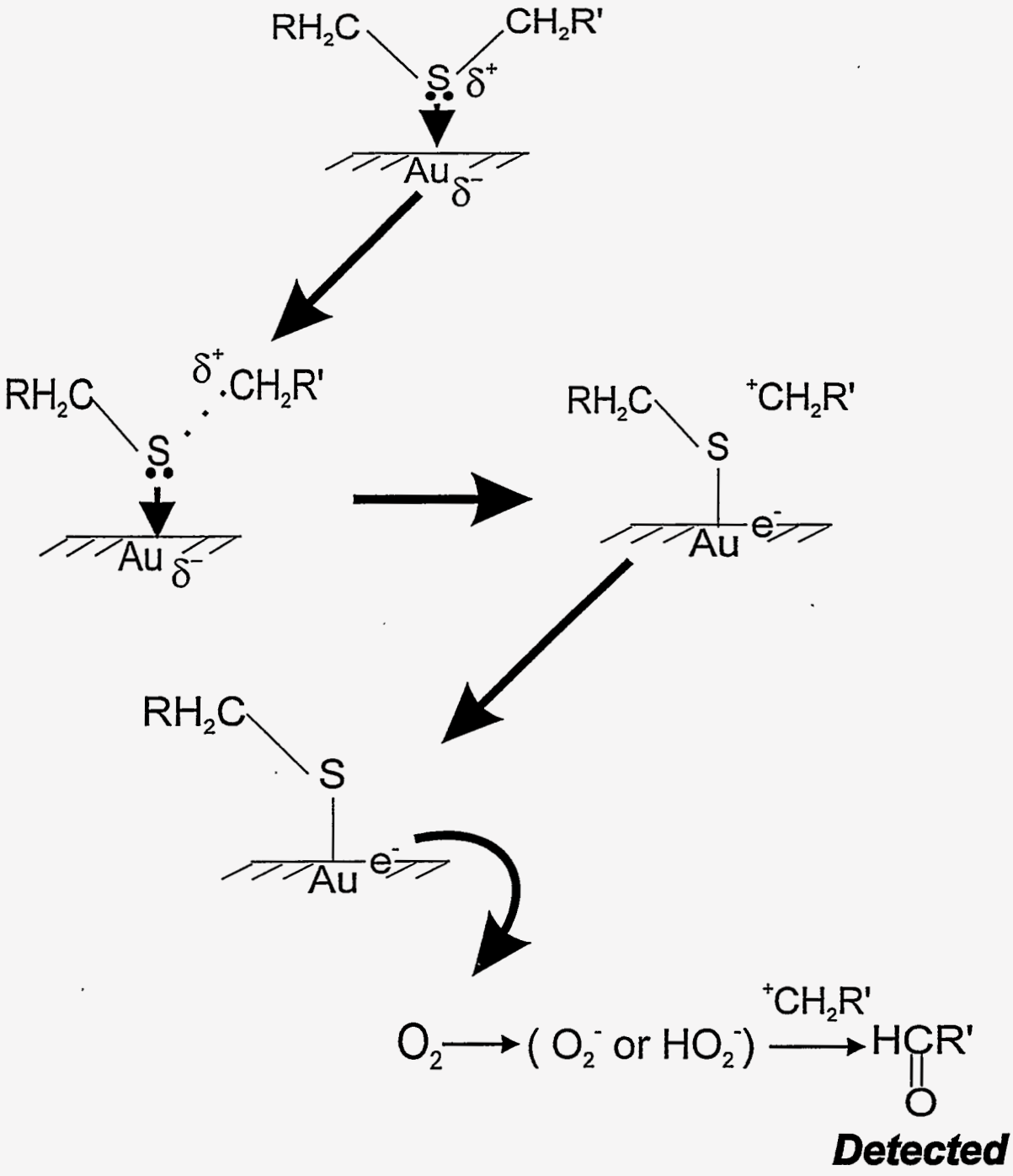

Figure 2.8: An adsorption mechanism for the formation of alkyl sulfides at gold electrodes

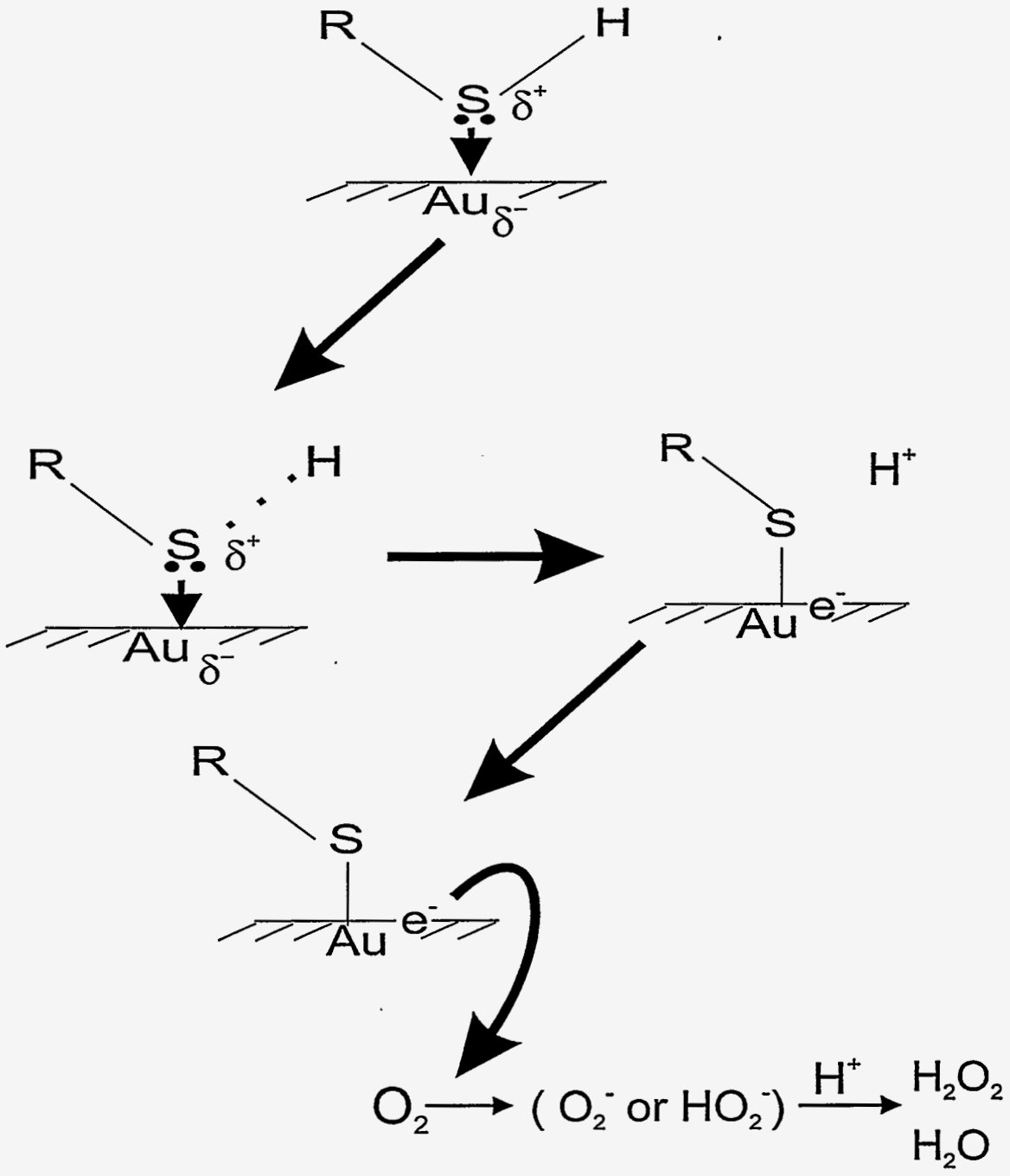

Figure 2.9: An adsorption mechanism for the formation of an alkyl thiol at a gold electrode.

sulfur donates electrons to gold, the partial positive charge generated on sulfur weakens the bond between sulfur and carbon for the alkyl sulfide and sulfur and hydrogen and eventually breaks. The buildup of charge density at the gold electrode can then be removed by oxygen-containing species. We are curently working to develop a mechanism for the formation of the aldehyde endgroup.

In closing, this study has presented XPS, IRS, GC-MS and electrochemical data which demonstrates that the monolayers formed from the four carbon analogs of thiols, sulfides and disulfides are essentially identical. We can assume this to be true for other chain lengths and studies to verify this are underway. Furthermore, we have derived mechanisms for the chemisorption of thiols and sulfides at gold, demonstrating that species containing oxygen are one of the possible sources in providing a route for the discharging of the electrode surface. These findings add to our present understanding of head group-substrate interactions that drive monolayer formation, and will prove critical in the design of monolayers for future applications.

Acknowledgements

The expert assistance of Jim Andregg with the XPS study is gratefully acknoledged. This work was supported by the Office of Basic Energy Sciences, Chemical Sciences Division.

References

1. Ulman, A. *An Introduction to Ultrathin Organic Films: From Langmuir-Blodgett to Self Assembly*, Academic: Boston, **1991**.

2. Hickman, J.J.; Oder, D.; Laibinis, P.E.; Whitesides, G.M.; Wrighton, M.S. *Science* **1991**, *252*, 688.

3. Jordan, C.E.; Frey, B.L.; Kornguth, S.; Corn, R.M. *Langmuir* **1994**, *10*, 3462.

4. Xu, C.; Sun, L.; Kepley, L.J.; Crooks, R.M.; Ricco, A.J. *Anal. Chem.* **1993**, *65*, 2102.

5. Allara, D.L.; Heburd, A.F.; Padden, F.J.; Nuzzo, R.G.; Falcon, D.R. *J. Vac. Sci. Technol.* **1983**, *1*, 376.

6. Green, J.-B.D.; McDermott, M.T.; Porter, M.D.; Siperko, L.M. *J.Phys Chem.* **1995**, *99*, 10960.

7. Frisbie, C.D.; Rozsnyai, L.F.; Noy, A; Lieber, C.M. *Science* **1994**, *265*, 2071.

8. Kumar, A.; Whitesides, G.M. *Appl. Phys. Lett.* **1993**, *63*, 2002.

9. Fenter, P.; Eberhardt, A.;Eisenberger, P. *Science* **1994**, *266*, 1216.

10. Gerdy, J.J.; Goodard, W.A. *J. Am. Chem. Soc.* **1996**, *118*, 3233.

11. Krysinski, P.; Chamberlain, R.V.; Majda, M. *Langmuir* **1994**, *10*, 4286.

12. Schneider, T.W.; Buttry, D.A. *J. Am. Chem. Soc.* **1993**, *115*, 12391.

13. Widrig, C.A.; Alves, C.A.; Porter, M.D. *J. Am. Chem. Soc.* **1991**, *113*, 2805.

14. Smith, E.L.; Porter, M.D. *J. Phys. Chem.* **1993**, *97*, 8032.

15. Walczak, M.M.; Popenoe, D.D.; Deinhammer, R.S.; Lamp, B.D.; Chung, C.; Porter, M.D. *Langmuir* **1991**, *7*, 2687.

16. Widrig, C.A.; Chung, C.; Porter, M.D. *J. Electroanal. Chem.* **1991**, *310*, 335.

17. Weisshaar, D.E.; Walczak, M.M.; Porter, M.D. *Langmuir* **1993**, *9*, 323.

18. Walczak, M.M.; Alves, C.A.; Lamp, B.D.; Porter, M.D. *J. Electroanal. Chem.* **1995**, *396*, 103.

19. McDermott, C.A.; McDermott, M.T.; Green, J.-B.; Porter, M.D. *J. Phys. Chem.* **1995**, *99*, 13257.

20. Zhong, C.J.; Porter, M.D. *J. Am. Chem. Soc.*; **1994**, *116*, 11616.

21. Hallmark, V.N.; Chiange, S.; Rabolt, J.F.; Swalen, J.D.; Wilson, R.J. *Phys. Rev. Lett.* **1987**, *59*, 2879.

22. Zei, M.S.; Nakai, Y.; Lehmpfuhl, G.; Kolb, D.M. *J. Electroanal. Chem.* **1983**, *150*, 201.

23. Walczak, M.M.; Chung, C.; Stole, S.M.; Widrig, C.A.; Porter, M.D. *J. Am. Chem. Soc.* **1991**, *113*, 2370.

24. Nuzzo, R.G.; Zegarski, B.R.; Dubois, L.H. *J. Am. Chem. Soc.* **1987** *109*, 733.

25. Bain, C.D.; Biebuyck, H.A.; Whitesides, G.M. *Langmuir* **1989**, *5*, 723.

3. STRUCTURAL CHARACTERIZATIONS OF CYCLIC ORGANOSULFUR-BASED MONOLAYERS: THE CASE OF THIOCTIC ACID

A paper to be submitted to *Langmuir*

Nina T. Woods, Chuanjian Zhong, Marc D. Porter

Introduction

The interest in monolayers fashioned from organosulfur molecules chemisorbed at gold has skyrocketed in recent years, not only because they are good models for interfaces, but also because of their potential utility in many technological areas. Of the many films formed from organosulfur species, monolayers formed from thiols [1-4] and disulfides [5-9] have been the most extensively studied. Nevertheless, the exact structure and interactions of gold sulfur bonding of these species remain elusive and controversial. Some recent reports [10-11] have challenged the general consensus that both thiols and disulfides form thiolate monolayers on the surface.

Of the disulfides, thioctic acid (1,2-dithiolane-3-pentanoic acid, see Figure 3.1) is particularly unique as a precursor for spontaneously adsorbed monolayers. The disulfide moiety of this asymmetric molecule is contained in a strained 5-membered ring. The structure of this molecule raises some interesting questions about the mechanism of its adsorption on the surface and may shed some insight

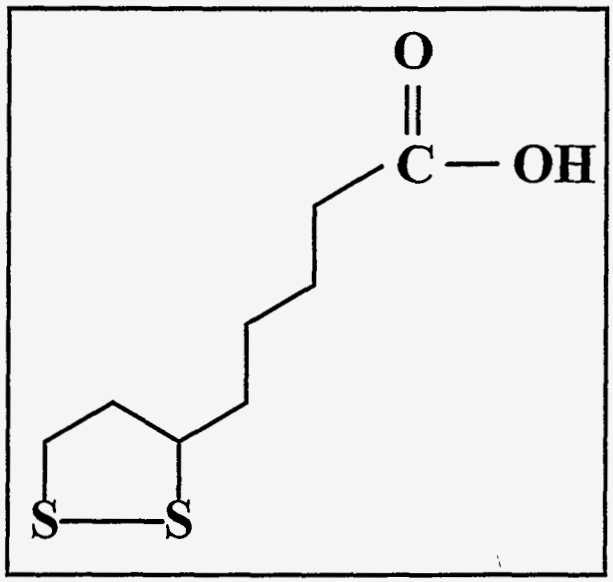

Figure 3.1: Structure of thioctic acid (1,2-dithiolane-3-pentanoic acid)

concerning the more general issues regarding the interactions of gold with organosulfur molecules. For example, does the S-S bond of the disulfide cleave upon chemisorption on gold as found with dialkyl disulfides [7,12]? If so, do both sulfurs form gold-bound thiolates after S-S cleavage, or does the ring strain prevent such bonding?

This chapter takes an in-depth look at thioctic acid monolayers formed at gold through characterizations by X-ray photoelectron spectroscopy (XPS), infrared reflection spectroscopy (IRS), cyclic voltammetry (CV) and scanning tunneling microscopy (STM). Based on the characterization results, a scheme for understanding the surface structure of thioctic acid monolayers is discussed. Sulfur-derived monolayers are widely used to improve the voltammetric responses of

biological molecules [13,14]. Thus, we have also assessed the feasibility of using thioctic acid monolayers to enhance cytochrome *c* electrochemistry.

Experimental

Materials

Potassium hydroxide (99.99%), thioctic acid (98%), sodium phosphate, potassium phosphate, and cytochrome *c* (horse heart muscle) were all obtained from Aldrich Chemical Company and used as received. Mercaptohexadecanoic acid and mercapotundecanoic acid were synthesized and purified according to established procedures [15].

Electrode Preparation

Electrodes were prepared by the resistive evaporation of gold onto either microscope glass slides (Fisher) or freshly cleaved mica using the following procedure.

Mica substrates (B&M Trading Company) were freshly cleaved into 75 mm x 25 mm sheets with a razor blade and passed under a stream of high purity argon prior to placement in the deposition chamber. Glass slides were cleaned in a 20% solution of Micro laboratory cleaner solution (Cole-Parmer), then rinsed with water and methanol and dried under a stream of argon prior to evaporation.

Depositions were performed using an Edwards (Wilmington, MA) E306A vacuum coater operating at a base pressure of 10^{-6} torr. A nominal thickness of 300

nm of gold was deposited onto the mica surface at an evaporation rate of 0.3 - 0.4 nm/s. The same procedure was followed for glass substrates, except that the glass was first primed with 15 nm of chromium.

Substrates were removed from the deposition chamber after cooling to ambient temperature. Upon removal, the Au/mica electrodes were annealed for 5 hours at 300°C in a muffle furnace under ambient atmosphere and allowed to cool to room temperature before storing in a dessicator. Glass substrates were used without annealing.

Monolayer Preparation

Gold electrodes were immersed in a 1 mM ethanolic solution of thioctic acid for 12 - 18 hours. Just prior to use, the electrodes were rinsed copiously with absolute ethanol, then dried on a spin coater (Headway Research Inc., Garland, TX)

Electrochemical Measurements

Cyclic voltammetric experiments were performed in a conventional three electrode electrochemical cell. The electrode area, defined by an inert elastomer O-ring, was 0.63 cm^2. A platinum coil electrode was used as a counter electrode. The reference electrode was a silver-silver chloride (saturated KCl) electrode. All potential measurements reported herein are given with respect to the latter electrode. Solutions were purged with high purity argon for at least 5 minutes just before data collection to remove oxygen.

Electrochemical data were collected using a BAS (Bioanalytical Systems, West Lafayette, IN) model CV-27 potentiostat coupled with an X-Y recorder (The Recorder Company).

Reductive desorption experiments of thioctic acid monolayers were performed in 0.5 M KOH electrolyte solutions. For the cytochrome *c* electrochemistry, a 10 mM phosphate buffer (pH 7) was used as the electrolyte.

X-Ray Photoelectron Spectroscopy (XPS)

XPS spectra were acquired using a Physical Electronics (Eden Prairie, MN) Model 5500 surface analysis system equipped with a hemispherical analyzer and torroidal monochrometer. A multichannel detector and 300W Kα radiation (1486.6 eV) was used for excitation. The detection angle was 45^0 from the surface normal.

Infrared Reflectance Spectroscopy (IRS)

Infrared spectra were obtained with a Nicolet Magna 750 FT-IR spectrometer fitted with a liquid nitrogen-cooled HgCdTe detector. Reflectance spectra were collected with *p*-polarized light incident at 80^0 from the surface normal. The spectra are presented as $-\log(R/R_0)$ where R is the reflectance of the sample and R_0 is the reflectance of an octadecanethiolate-d_{37} monolayer on Au. Details concerning the preparation and handling of reference substrates have been previously given [16].

Scanning Tunneling Microscopy (STM)

STM images were obtained with a Digital Instruments Nanoscope III (Santa Barbara, CA) equipped with a 0.7 μm scan head. The instrument was operated under ambient conditions and allowed to equilibrate thermally for ~30 minutes after loading the samples. The images were acquired in constant height mode and software flattened.

The STM tips were made by electrochemically etching 0.25 mm tungsten wire (Aldrich) in 1 M KOH (99.99%, Aldrich) at 30 V ac. A tip was discarded if well defined images were not obtained after scanning several regions of a sample. Bias voltages were typically 900 mV with respect to the sample. The tunneling current was ~500 pA.

Cytochrome c Adsorption

After thioctic acid monolayers were formed on Au/glass, the slides were removed from the precursor solution, rinsed with ethanol and dried. These slides were subsequently immersed in 30 μM cytochrome *c* in a phosphate buffer (pH 7, 10 mM ionic strength). The cytochrome *c* solution was kept at ~0^0 during the adsorption process. Prior to the electrochemical experiments, the slides were rinsed thoroughly with phosphate buffer after removal from the cytochrome *c* solutions.

Results and Discussion

Characterizations of the As-formed Monolayer

Infrared reflection spectroscopy was utilized to examine these monolayers. Figure 3.2 presents the data in both the high and low frequency region. The high frequency region contained peaks at 2934 cm^{-1} and 2864 cm^{-1} corresponding to the asymmetric and symmetric stretches of the methylene groups respectively [17] The strong absorption band at 1719 cm^{-1} corresponds to the C=O stretch for hydrogen-bonded carboxylic acid end groups [17].The peaks at 1418 cm^{-1} and 1280 cm^{-1} are assigned to the O-H bending and C-O stretching, respectively [17]. The peak at 920 cm^{-1} results from the out-of-plane bending of the bonded O-H in the dimer [17]. These data are consistent with the expected composition for thioctic acid monolayers.

Figure 3.3 shows the XPS spectra of a monolayer derived from thioctic acid in the S(2p) region following 18 hours of immersion in a 1 mM formation solution of precursors. Although not shown, the XPS spectra for carbon and oxygen are consistent with the expected composition of the monolayer. In comparison with the XPS spectra for thiol and disulfide-based monolayers whereby a single set of peaks representing the sulfur $2p_{3/2}$ and $2p_{1/2}$ couplet are observed, three peaks are evident in the same energy region for thioctic acid monolayers. Upon deconvolution [18], the presence of two sets of the 2p couplet reveals the existence of two different sulfur species. The 2p couplet at 161.7 eV and 162.9 eV has previously been ascribed to

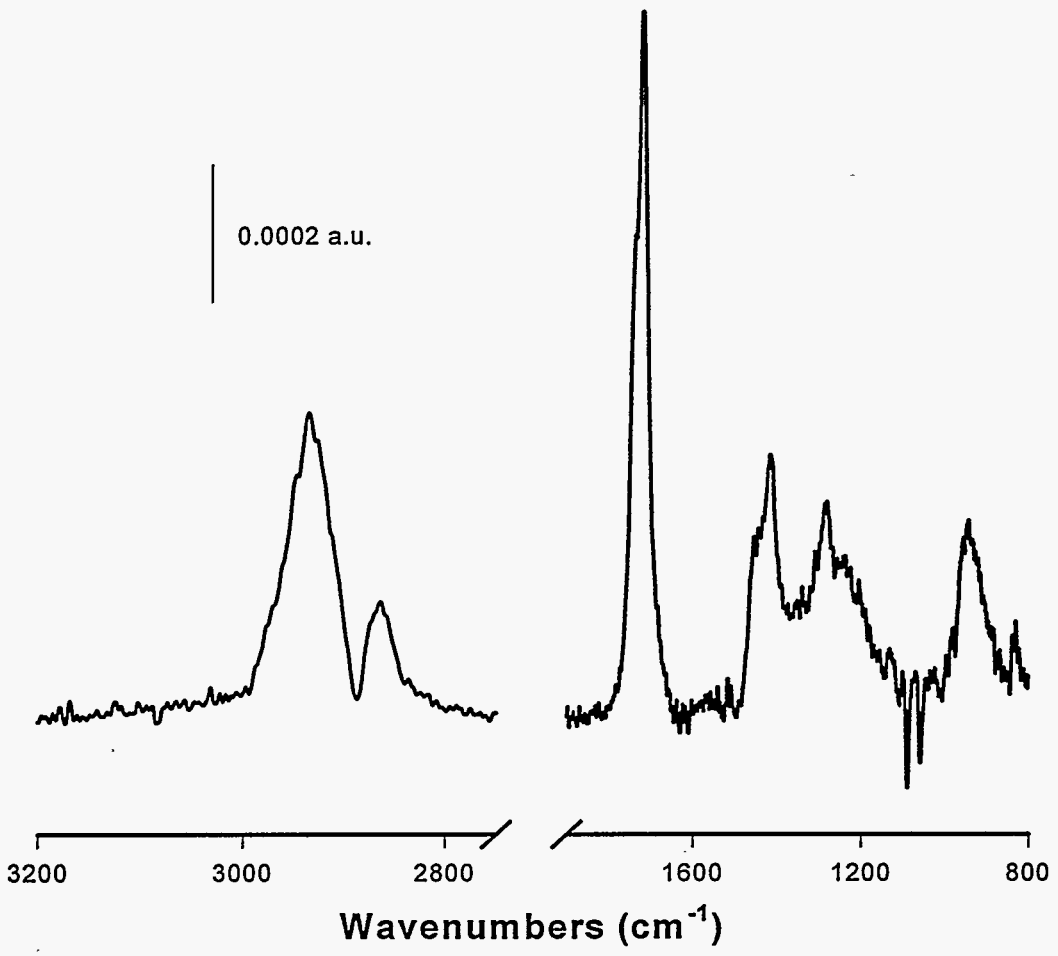

Figure 3.2: IRS spectrum in the 2000 - 600 cm^{-1} region of a monolayer derived from thioctic acid.

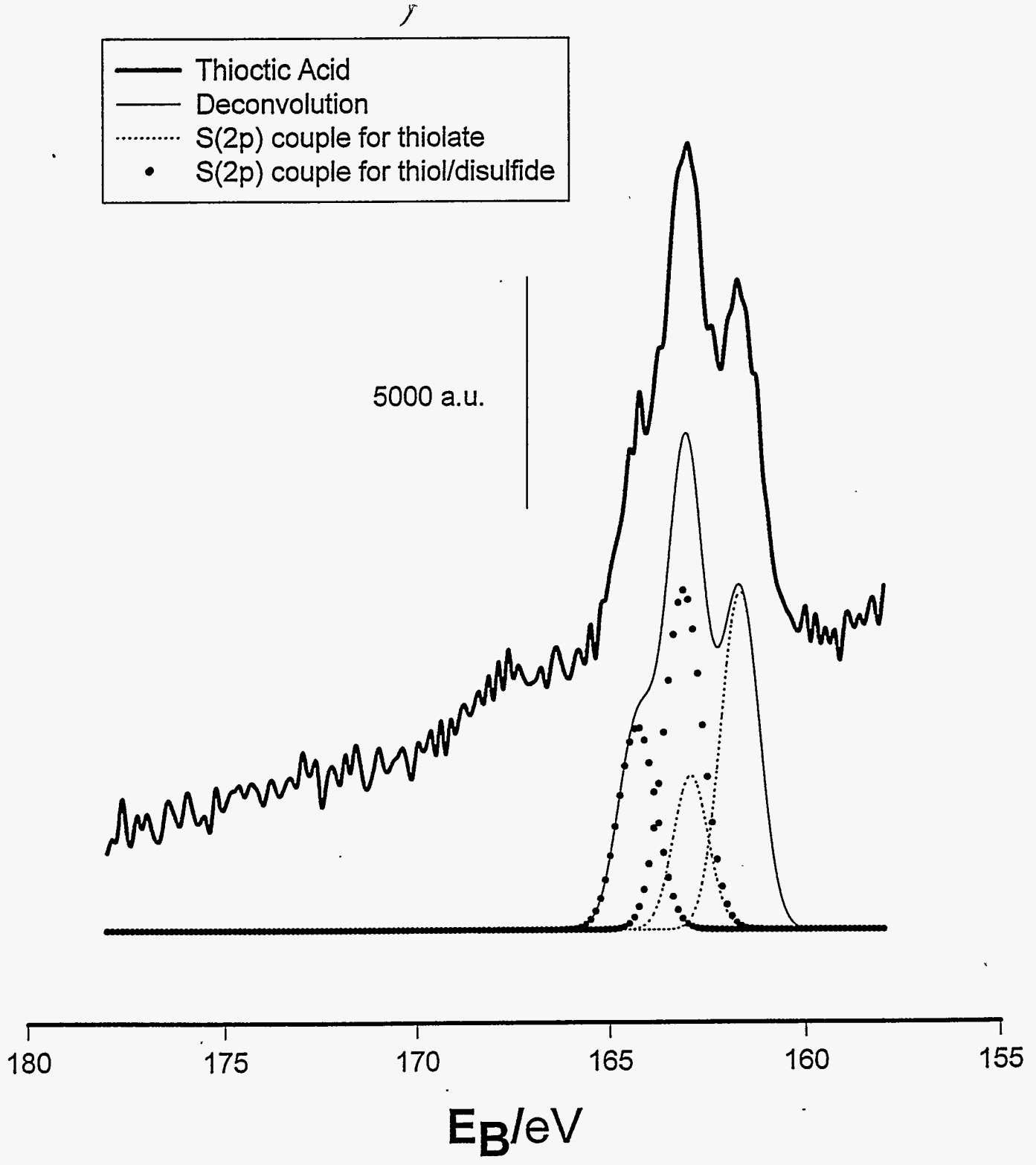

Figure 3.3: XPS spectrum of thioctic acid in the sulfur 2p region. The lower set of curves represent the deconvolution of the thioctic acid spectrum.

a gold-bound thiolate [5,19]. The higher energy couplet at 163.2 eV and 164.5 eV, however, is more diagnostic of either a free thiol or free disulfide [20]. Based on an analysis of the peak intensity of the two species, the thiolate is as prevalent on the surface as the higher binding energy species. Thus, as a preliminary indication, the XPS results argue that the S-S bonds for half of the thioctic acid molecules are cleaved to form thiolates on the surface. However, the results also reveal the possibility that some of the immobilized species exist as either uncleaved disulfides and/or as thiols, the latter of which would reflect cleavage of the disulfide bond to yield a gold-bound thiolate and a thiol.

The thioctic acid monolayers were further characterized by reductive desorption voltammetry. The cyclic voltammogram in Figure 3.4 shows a rather broad cathodic wave at a potential of -0.92 V representing the desorption of the monolayer. The reverse wave represents the redeposition of material captured from the diffusion layer. The peak position of the wave is consistent with a mercaptoalkanoic acid of a chain length between 5 carbons (E_p = -0.82V) and 11 carbons (E_p = -0.95 V) [21]. The charge obtained by integrating the area under the cathodic wave, is 125 ($\pm$ 14.4) $\mu C/cm^2$. This charge is higher than what would be expected for a densely packed monolayer of alkanethiolates [22]. However, we believe this charge is not indicative of a greater surface coverage. Some possible contributions to the charge flow of the reductive desorption process include dipole moment effects of the end group, as observed with dithiol species [23] and/or the possible direct

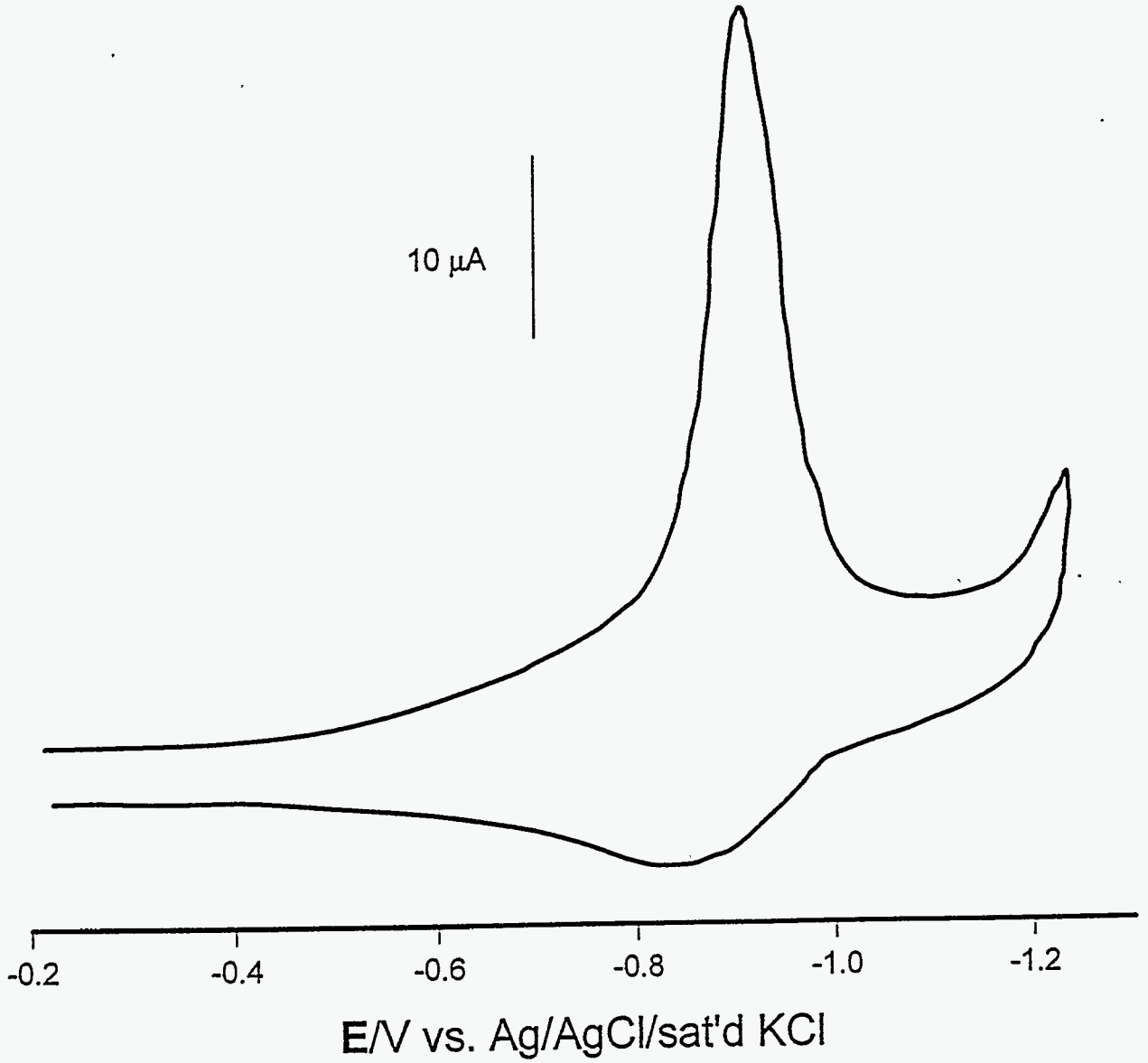

Figure 3.4: Cyclic voltammogram of a monolayer derived from a 1 mM solution of thioctic acid. The electrolyte was 0.5 M KOH and the scan rate was 50 mV/s.

electrochemical reduction of the free SH group , as shown in the following equation:

$$R\text{-}SH + e^- \rightarrow RS^- + \tfrac{1}{2} H_2$$

The STM image of a thioctic acid monolayer (Figure 3.5) shows a high density of pits, roughly 30% of the surface area. These defects have previously been observed on monolayers formed from straight-chain dialkyl disulfides [12]. This study also showed that the S-S bonds in straight-chain dialkyl disulfides cleave to form thiolates. Thus, the similarity between the straight-chain and cyclic disulfides supports the theory that the S-S bond in thioctic acid cleaves as well to form gold-bound thiolates on the surface.

The characterization of thioctic acid monolayers testifies that these surfaces are more structurally complicated than monolayers formed from straight chain alkyl thiols or dialkyl disulfides. Preliminary evidence indicates that thioctic acid precursors form two or more different sulfur species as a result of its spontaneous adsorption onto gold. The next section describes a scheme to pinpoint the type of sulfur species present on the surface.

Characterizations based on surface-derivatization

The characterization of the monolayer up to this point shows the possibility of two or more sulfur species present at the surface of the electrode. Figure 3.6 shows four idealized structural possibilities for the thioctic acid monolayer.

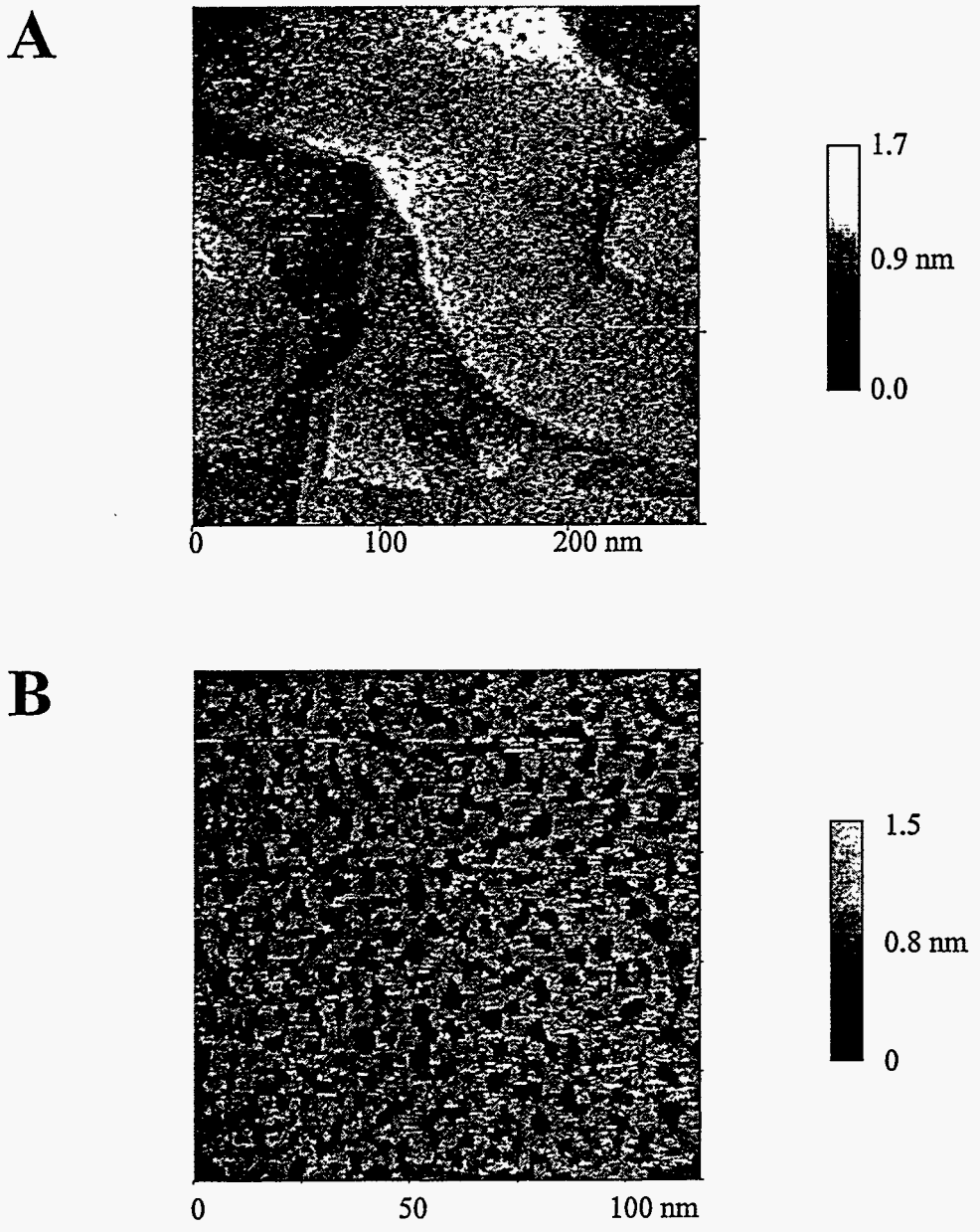

Figure 3.5: STM images of thioctic acid. A) A 270 nm image collected with bias voltage of 900 mV and setpoint of 500 pA. B) A 117 nm image collected with bias voltage of 900 mV and setpoint of 200 pA.

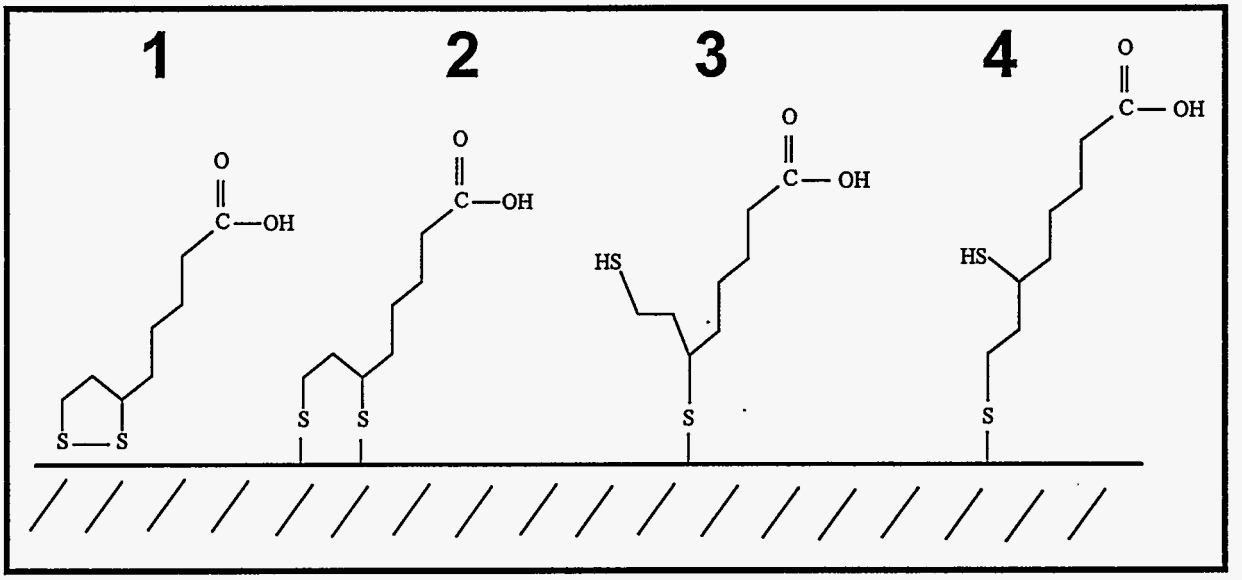

Figure 3.6: Conformation possibilities for sulfur species formed from thioctic acid at a gold electrode.

Species 4 is the analog of species 3, depending on which sulfur atom is attached to gold as a thiolate. Interestingly, space-filling modeling supports the possibility of both sulfurs binding at the $\sqrt{3}$ spacing for nearest neighbors observed for alkanethiolates monolayers at Au(111). We have not, however, attempted to determine packing density limits for any of the possibilities.

Based on the possible presence of species 3 and 4, we attempted to detect the existence of free thiols using the acid chloride reaction scheme shown in Figure 3.7. Since the direct addition of acetyl chloride to thioctic acid would produce an anhydride, the carboxylic acid group was first blocked by esterification [24]. The ester-functionalized form was then spontaneously adsorbed onto the gold surface. The resulting monolayer was subsequently exposed to acetyl chloride vapors for 1 hour and rinsed with absolute ethanol before analyses.

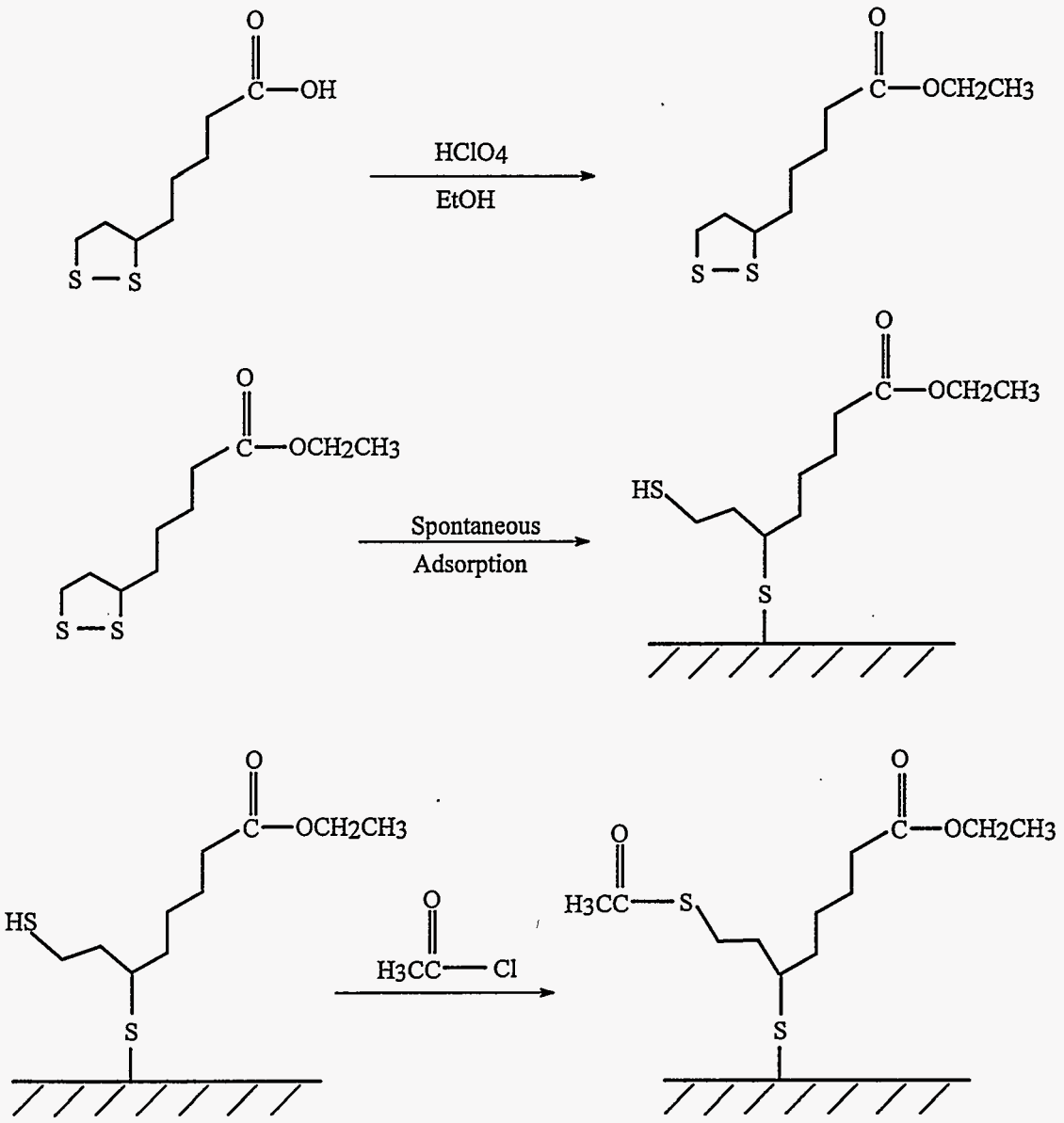

Figure 3.7: Reaction schematics for the derivatization of thioctic acid to an ethyl ester and the subsequent reaction with acetyl chloride

Figure 3.8 shows the XPS in the S(2p) region and IRS data in the low-frequency region for monolayers formed from the ethyl ester derivatives of thioctic acid. The IRS spectrum shows a peak at 1740 cm^{-1} which corresponds to the ester [18]. This result confirms the formation of the ethyl ester derivative by the shift of the C=O band to higher energy in comparison to that in Figure 3.3 for the hydrogen bonded carboxylic acids. The ratio of the higher binding energy XPS S(2p) peaks to the lower energy component in the two monolayers were calculated by deconvoluting the peaks (as in Figure 3.3) and integrating the areas under the peaks for each component. The ratio for the monolayer formed from the functionalized ethyl ester precursor is 1.8, relatively larger than that of the thioctic acid monolayer (1.1). We attribute this to the possibility that a greater amount of disulfide bonds were cleaved in the ester-derivatized form, probably due to the presence of excess protons in the monolayer formation solution [12].

The analogous IRS and XPS spectra for the ester-functionalized monolayer after exposure to acetyl chloride vapor is shown as Figure 3.9. The XPS S(2p) spectra indicates a significant degradation of the derivatized thioctic acid species. This loss may be the result of excessive rinsing of the samples or a weakened Au-S bond as a result of the derivatization. However, in the IRS spectra, there is a small shoulder of the ester peak around 1690 cm^{-1} that corresponds to ν(C=O) as a result of the reaction of acetyl chloride with the thiol group [27]. These preliminary results suggest the presence of free thiol groups at the monolayer surface.

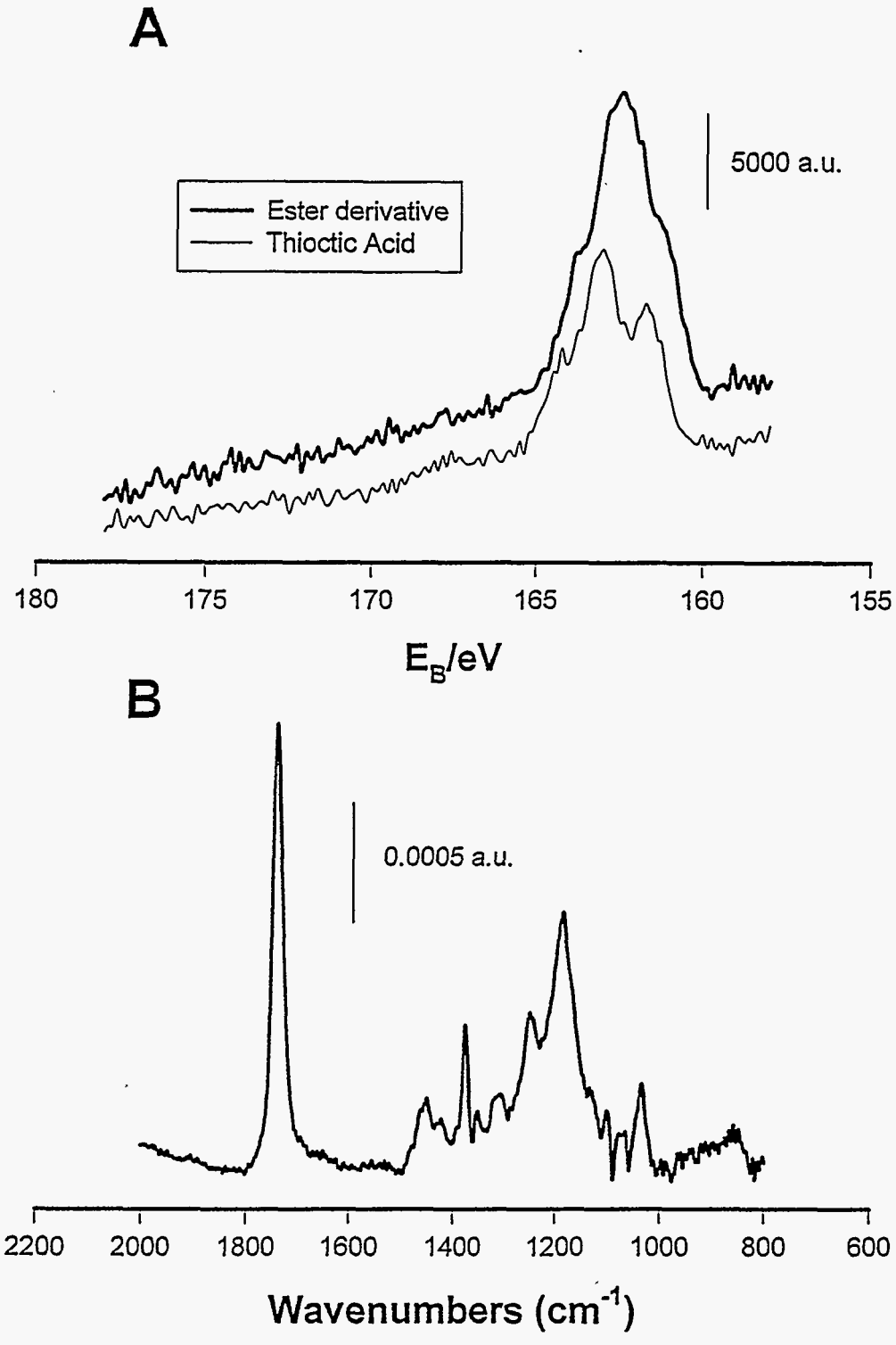

Figure 3.8: A) XPS spectrum in the S(2p) region for the ester derivative of thioctic acid. The original spectrum for thioctic acid in the same region is redrawn here for comparison. **B)** IRS spectrum of the ester derivative of thioctic acid.

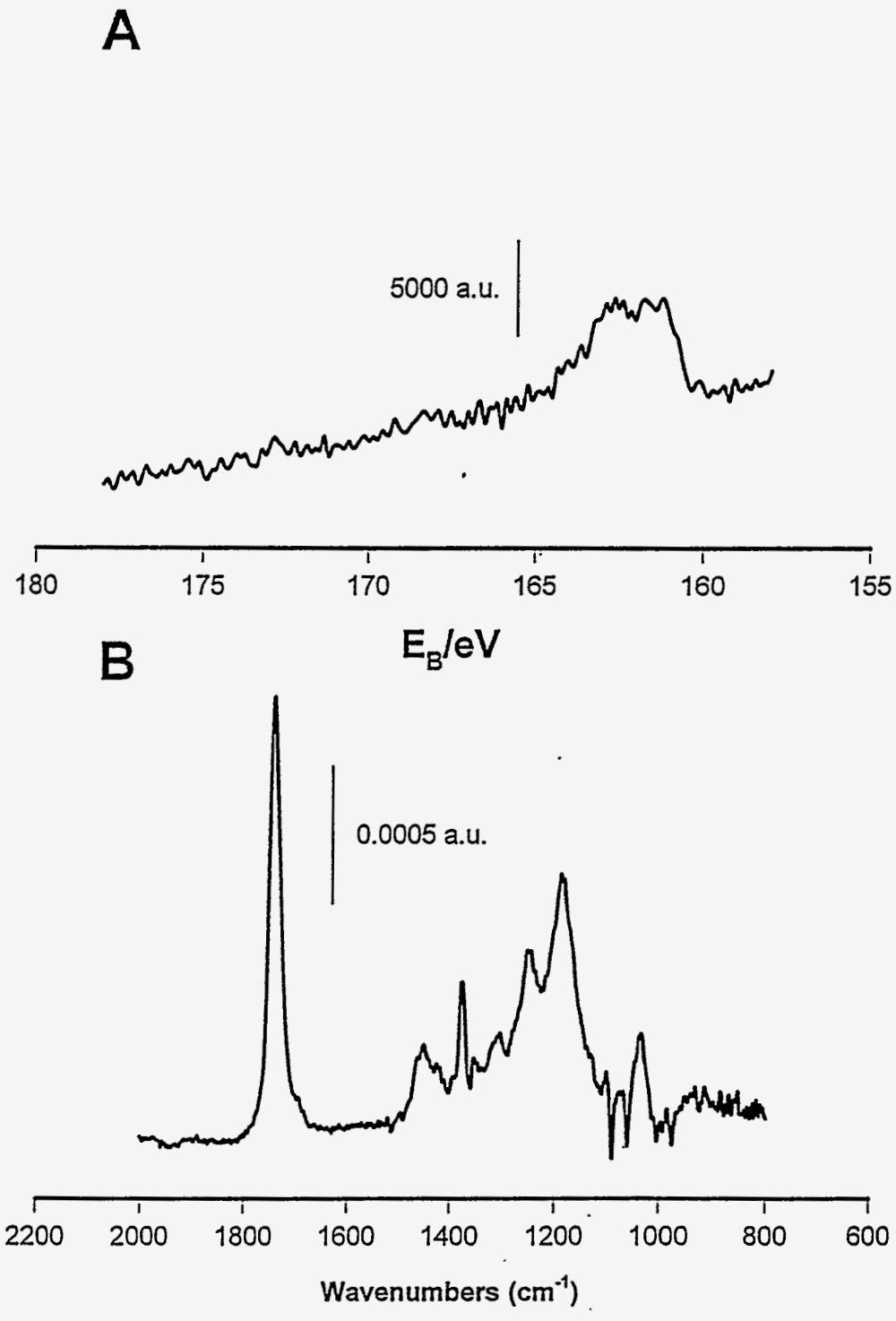

Figure 3.9: A) XPS spectra in the S(2p) region of a monolayer of ester-derivatized thioctic acid after reaction with acetyl chloride. B) IRS spectra of the same species in the region from 2000 - 800 cm^{-1}.

In summary, the derivatization of the carboxylic acid group of the thioctic acid to an ester was partially successful. The IRS data show the presence of an ester moiety and XPS spectra in the sulfur region verify that there are thiolates on the gold surface. Due to yet unknown causes, the reaction of the ester-derivatized monolayer with acetyl chloride resulted in the loss of some sulfur species. However, IRS results suggest that a small amount of free thiol groups exist. It is possible that not all of the molecules are able to find binding sites for both sulfurs. Thus, some of the molecules assemble with one sulfur atom attached to gold and the other sulfur as a free thiol, as suggested by the presence of the higher binding energy S(2p) component of the XPS spectra.

Applications to Cytochrome c Electrochemistry

Thioctic acid monolayers have been used in the study of electron transfer distance relationships [28] and in immobilization of antibodies for enzyme immunoassays [29]. As another example of the utility of these monolayers, we demonstrate in this section the feasibility of using these thioctic acid monolayers to improve cytochrome *c* voltammetry. It is known that large biological molecules such as cytochrome *c* have poor electrochemical responses at bare electrodes. By modifying the surface of the electrode, rapid electron transfer can be attained between the biological molecule of interest and electrode. A number of other organosulfur species have already been tested as molecular "anchors" for cytochrome *c* [13,14,30,31]. In particular, Song, et. al. have extensively

characterized straight chain mercaptoalkanoic acids for this purpose [31]. Our goal was to determine if cyclic disulfides such as thioctic acid were equally effective at promoting cytochrome *c* electron transfer as these straight chain mercaptoalkanoic acids.

The CV of cytochrome *c* immobilized at three different monolayers: thioctic acid, mercaptohexanoic acid and mercaptoundecanoic acid, is shown in Figure 3.10. The latter two species have already been studied by Song et. al [31]; the electrochemical experiments were repeated here for comparison with thioctic acid derived monolayers. In all three cases, the cyclic voltammogram in the potential window from 0.4 to -0.2 V in the absence of cytochrome *c* reflected only the double layer charging current. Table 3.1 summarizes the electrochemical behavior of these modified electrode (TA).

Table 3.1: Summary of the Electrochemical Behavior of Immobilized Cytochrome *c* at Acid-Terminated Monolayers

	C_{dl} ($\mu F/cm^2$)	Γ ($pmol/cm^2$)	$E^{0'}$ (mV vs Ag/AgCl)	ΔE_p (mV)
16-MHDA	3.2	2.4	30	150
11-MUDA	8	10	30	20
TA	17	7.0	50	10

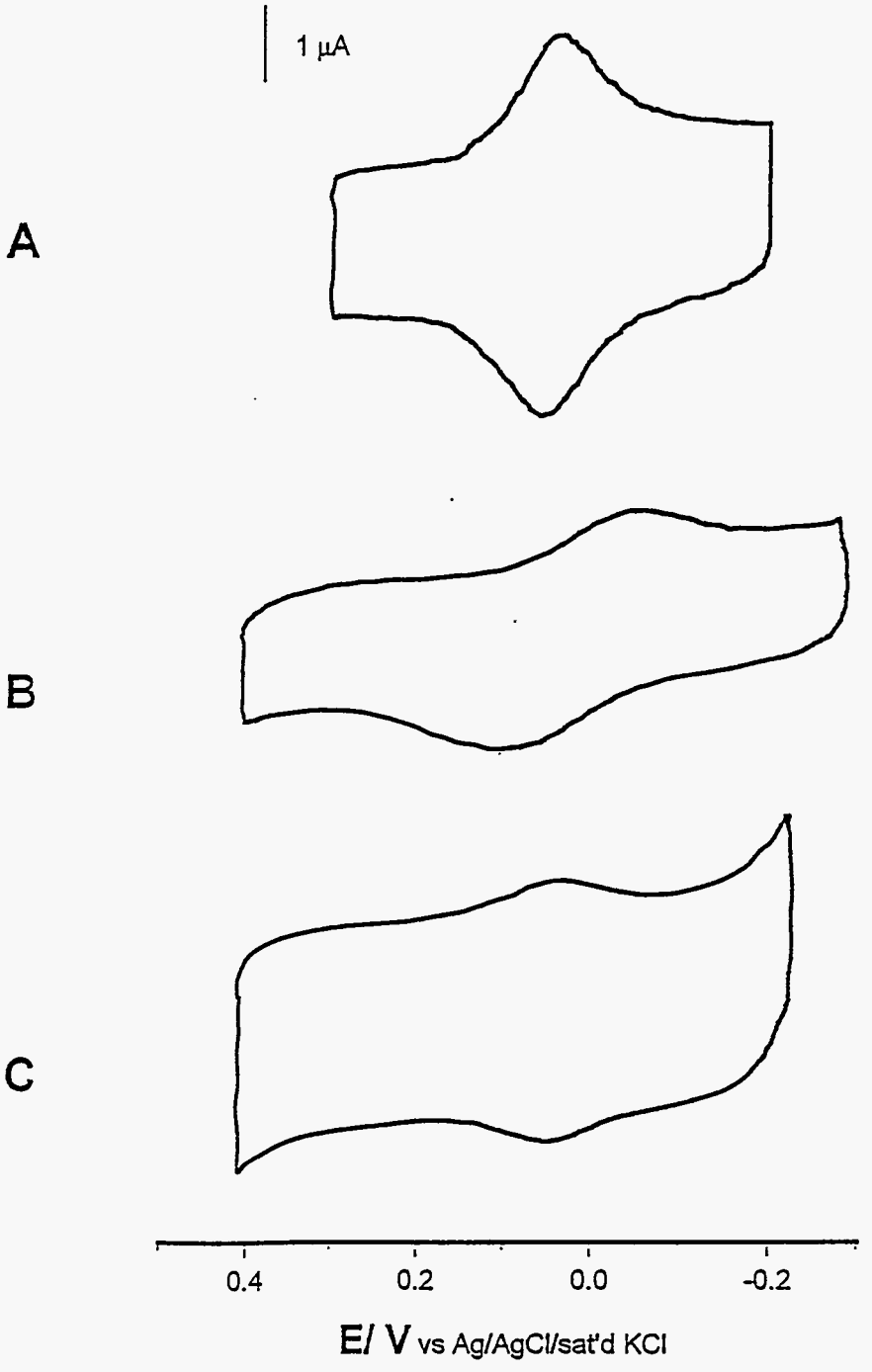

Figure 3.10: Cyclic voltammogram of cytochrome *c* immobilized on **A)** mercaptoundecanoic acid, **B)** mercaptohexadecanoic acid and **C)** thioctic acid. The electrolyte is a pH 7, 10mM ionic strength phosphate buffer. The CV was collected at a scan rate of 50 mV/s

The double layer capacitance was calculated by the following equation:

$$C_{dl} = (i_c + i_a)/ 2\nu A$$

where i_c and i_a represent the cathodic and anodic currents (mA) in a region devoid of expected fardadaic processes, ν represents the scan rate (mV/s) and A represents the geometric electrode area (cm^2). In comparison to mercaptoalkanoic acids, the thioctic acid monolayer has a greater capacitance. This is consistent with the observation that as chain length decreases, capacitance increases because short alkyl chains are less well packed than longer chain monolayers. The surface coverage of 7 pmol /cm^2, calculated by integrating the area under the cathodic peak [22], is consistent with cytochrome *c* coverages at mercaptoundecanoic acid. The peak position ($E^{0'}$) for cytochrome *c*/thioctic acid/Au composite electrodes are also consistent with the mercaptoalkanoic acids. This value was derived by taking the average value of the cathodic peak position and anodic peak position ($(E_{p,c} + E_{p,a})/2$). In contrast, thioctic acid monolayers show more reversible character than the 11 or 16 carbon chain alkanoic acids.

The difference between cathodic and anodic peak potentials (ΔE_p) shows that monolayers derived from thioctic acid are more reversible than 16-MHDA and 11-MUDA. The fact that ΔE_p is so close to zero also indicates that the voltammetric waves observed are the result of a surface process. A scan rate dependence of the cytochrome *c*/ thioctic acid/ Au system also verifies the existence of a surface confined redox process. The results in Fig. 3.11 shows a linear dependence of peak

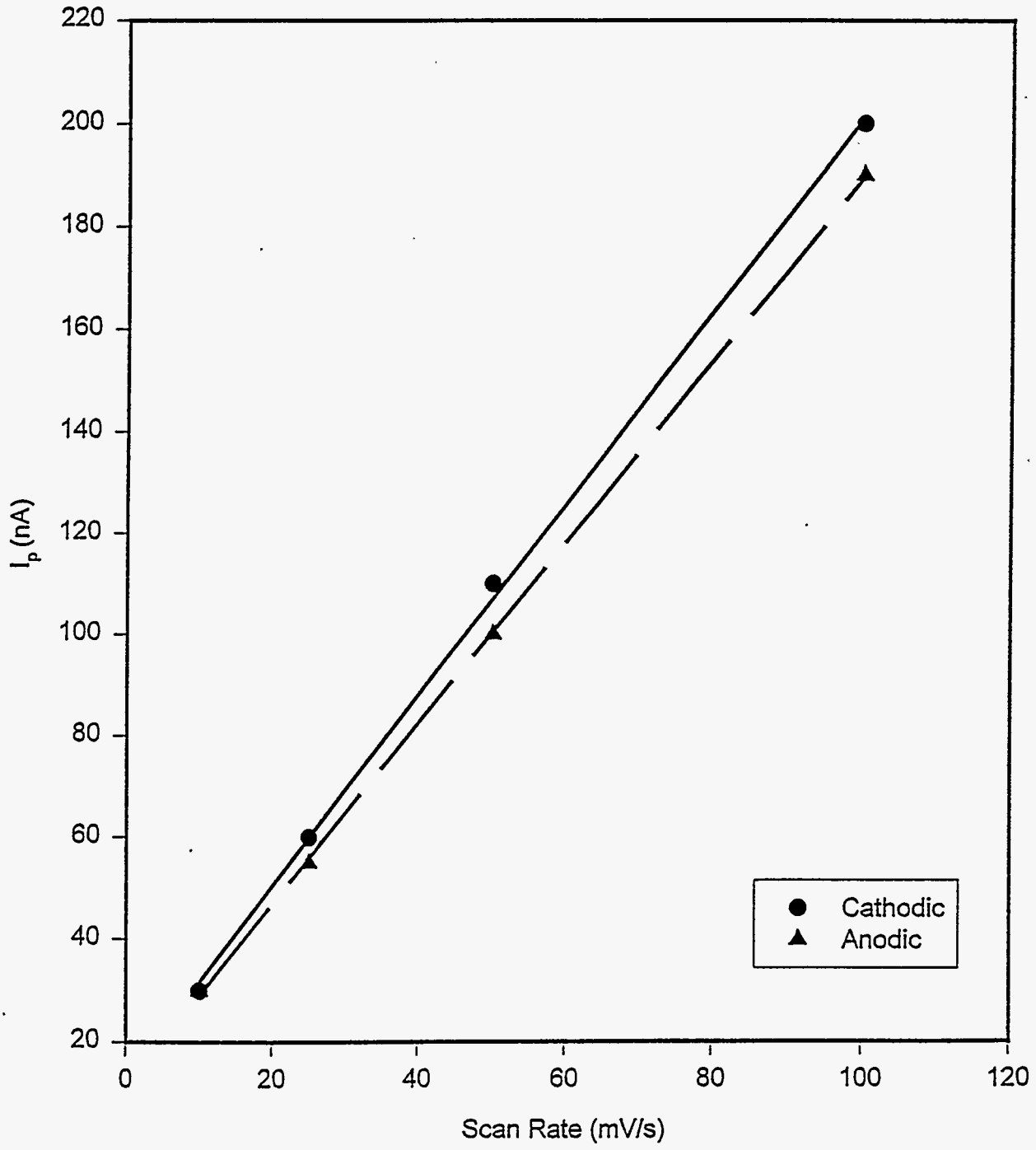

Figure 3.11: Scan Rate Dependence of the cytochrome *c*/ thioctic acid/Au composite electrode. The linear dependence of peak current on scan rate shows that the cytochrome *c* is immobilized on the surface.

current on scan rate and confirms that cytochrome *c* is a surface-attached redox species.

Thus, we have shown that thioctic acid can be used in the same manner as other mercaptoalkanoic acids to immobilize cytochrome *c* with comparable results despite the relative disorder of the surface species. Because of the relatively large size of this protein, it is likely that the effectiveness of electron transfer is unaffected by the monolayer structure.

Conclusions

The characterization of monolayers based on thioctic acid precursors is considerably more complicated than straight chain alkyl thiols or disulfides because of the shape of the thioctic acid molecule. There is experimental evidence for at least two different sulfur species, one of them being thiolates formed from the S-S bond cleavage of the disulfide. The preliminary data also indicates the possibility of a species whereby one sulfur atom is anchored to gold and the other sulfur atom is a free thiol group. This is likely to occur if the approaching thioctic acid molecule cannot find equivalent binding sites for both sulfur atoms at the surface. At this time, however, we cannot rule out the possibility of disulfides on the surface.

Another approach to determining the structural conformation of the surface species may involve the formation of monolayers using cyclic disulfides without the acid terminated alkyl chain. If it is true that the cleavage of the S-S bond causes the formation of a free thiol, the characteristics of this monolayer should be comparable

to monolayers derived from dithiols of the same chain length. Studies along this avenue are underway.

Despite the complications in determining the species at the surface, we have been successful at utilizing thioctic acid for the immobilization of cytochrome *c,* with comparable results to that of the other mercaptoalkanoic acids.

Acknowledgements

The expert assistance of Jim Anderegg in the collection of XPS data, and Sze-Shun Wong in the collection of STM data is gratefully acknowledged. This work was supported by the Office of Basic Energy Sciences, Chemical Science Division.

References

1. Porter, M.D.; Bright, T.B.; Allara, D.L.; Chidsey, C.E.D. *J. Am. Chem. Soc.* **1987**, *109*, 3559.

2. Whitesides, G.M.; Laibinis, F.E. *Langmuir* **1990**, *6*, 87.

3. Nuzzo, R.G.; Dubois, L.H.; Allara, D.L. *J. Am. Chem. Soc.* **1990**, *112*, 558.

4. Bain, C.D.; Troughton, E. B; Tao, Y.-T.; Evall, J.; Whitesides, G.M.; Nuzzo, R.G. *J. Am. Chem. Soc.* **1989**, *111*, 321.

5. Bain, C.D.; Biebuyck, H.A.; Whitesides, G.M. *Langmuir* **1989**, *5*, 723.

6. Nuzzo, R.G.; Allara, D.L. *J. Am. Chem. Soc.* **1983**, *105*, 4481.

7. Nuzzo, R.G.; Zegarski, B.R.; Dubois, L.H. *J. Am. Chem. Soc.* **1987**, *109*, 733.

8. Nuzzo, R.G.; Fusco, F.A.; Allara, D.L. *J. Am. Chem. Soc.* **1987**, *109*, 2358.

9. Hagenhoff, B.; Benninghoven, A.; Spinke, J.; Leley, M.; Knoll, W. *Langmuir* **1993**, *9*, 1622.

10. Gerdy, J.J.; Goodard, W.A. *J. Am. Chem. Soc.* **1996**, *118*, 3233.

11. Krysinski, P.; Chamberlain, R.V.; Majda, M. *Langmuir* **1994**, *10*, 4286

12. Lamp, B.D.; Franek, J.E.; Alves, C.A.; Porter, M.D., manuscript in preparation.

13. Eddowes, M.J.; Hill, H.O.A *J. Chem. Soc., Chem. Commun.* **1977**, 771.

14. Allen, P.A.; Hill, H.A.O.; Walton, N.J. *J. Electroanal. Chem.* **1984**, *178*, 69.

15. Bain, C.D.; Troughton, E. B; Tao, Y.-T.; Evall, J.; Whitesides, G.M.; Nuzzo, R.G. *J. Am. Chem. Soc.* **1989**, *111*, 321. (Supplementary material)

16. Walczak, M.M.; Chung, C.; Stole, S.M.; Widrig, C.A.; Porter, M.D. *J. Am. Chem. Soc.* **1991**, *113*, 2370.

17. Silverstein, R.M.; Bassler, G.C.; Morrill, T. C. *Spectrometric Identification of Organic Compounds* John Wiley and Sons: New York, **1991**.

18. Zhong, C.J.; Porter, M.D. *J. Am. Chem. Soc.* **1994**, *116*, 11616.

19. Smith, E.L.; Porter, M.D. *J. Phys. Chem.* **1993**, *97*, 8032.

20. Lindberg, B.J.; Hamrin, K.; Johansson, G.; Gelius, U.; Fahlman, A.; Nordling, C.; Siegbahn, K. *Phys. Script.* **1970**, *1*, 286.

21. Simmons, N.J.; Porter, M.D., unpublished results.

22. Widrig, C.A.; Chung, C; Porter, M.D. *J. Electroanal. Chem.* **1991**, *310*, 335.

23. Zhong, C.J.; Porter, M.D., manuscript in preparation.

24. The esterification procedures is as follows: An excess of 70% perchloric acid was added to 1 mM of thioctic acid in absolute ethanol. The resulting solution was stirred for 1 hour and gold slides were immersed into the solution to form the esterified monolayer.

25. Parker, A.J.; Kharasch, N. *Chem. Rev.* **1959**, *59*, 591.

26. Nakanishi, K.; Solomon, P.H. *Infrared Absorption Spectroscopy* Holden-Day: Oakland, **1977**, 43.

27. Feng, Z.Q.; Imabayashi, S.; Kakiuchi, T.; Niki, K. *J. Electroanal. Chem.* **1995**, *394*, 149.

28. Li, T. T-T.; Weaver, M.J. *J. Am. Chem. Soc.* **1984**, *106*, 6107.

29. Duan, C.; Meyerhoff, M.E. *Anal. Chem.* **1994**, *66*, 1369.
30. Taniguchi, I.; Toyosawa, K.; Yamaguchi, H.; Yasukouchi, K. *J. Electroanal. Chem.* **1972**, *140*, 187.

31. Song, S.; Clark, R.A.; Bowden, E.F.; Tarlov, M.E. *J. Phys. Chem.* **1993**, *97*, 6564.

4. GENERAL CONCLUSIONS

This thesis has provided several insights into the head group-substrate interactions which add to the foundation of knowledge related to organosulfur monolayers at gold surfaces.

We have established that butanethiol, butyl sulfide and butyl disulfide form the same thiolate monolayer on the surface and in the process, the S-H, S-C and S-S bonds, respectively, are cleaved. Furthermore, dissolved oxygen in solution plays an integral part in the mechanism by which these organosulfur species spontaneously adsorb on the surface.

The case of asymmetric, cyclic disulfides such as thioctic acid is considerably more complicated. Our results indicate that there are at least two possible conformations for the species on the surface, contributing to a monolayer that is not as organized or well-packed as its straight-chain counterparts. Despite complications in determining the exact nature of the adsorbate, thioctic acid monolayers have proven equally useful as other surface modifiers for the promotion of cytochrome *c* electrochemistry.

A better understanding of the interactions between sulfur and gold is essential for greater manipulation of monolayer formation and structure. Specifically, it would be interesting to examine precursors of other chain lengths to verify that the same thiolate monolayer forms. An in-depth study of the differences in the packing

and order of the chains within these monolayers will also be valuable to elucidate the exact structure formed from each precursor.

Thioctic acid holds promise for applications requiring electron transfer mediators and further studies along this avenue are warranted. A greater understanding of the orientation with which thioctic acid adsorbs on the surface will also lead to a better ability to predict the monolayer structure formed from other precursors.

Organosulfur monolayers have already contributed to a wide array of technological advances. The continued development of characterization methods and applications for these films will play a vital role in the progress of this field.

ACKNOWLEDGEMENTS

This work would not have been possible without the support of many people. First, I would like to thank my major professor Marc Porter for his leadership, guidance and encouragement. Special thanks also goes to CJ Zhong, whose assistance in this research was invaluable. To all the Porter Group members, thanks for many insightful discussions, work-related and otherwise! Last but certainly not least, I am grateful for the love and patience of my husband Shawn, who always stood by me through the difficult times, rejoiced with me when the going was good and most of all, kept me sane! Shawn, this thesis is as much yours as it is mine and even though you've never taken any chemistry classes, I could not have done this without you.

I also acknowledge the receipt of a Graduate Assistance in Areas of National Need (GAANN) fellowship during my first year. This work was performed at Ames Laboratory under Contract No. W-7405-Eng-82 with the U.S. Department of Energy. The United States government has assigned the DOE Report number IS-T1789 to this thesis.